CHEMICAL REVIEWS

Review

pubs.acs.org/CR

From Widely Accepted Concepts in Coordination Chemistry to Inverted Ligand Fields

Roald Hoffmann,*[,†] Santiago Alvarez,[‡] Carlo Mealli,[§] Andrés Falceto,[‡] Thomas J. Cahill, III,[∥] Tao Zeng,[⊥] and Gabriele Manca[§]

[†]Department of Chemistry and Chemical Biology, Baker Laboratory, Cornell University, Ithaca, New York 14853, United States

[‡]Departament de Química Inorgànica and Institut de Química Teòrica i Computacional, Universitat de Barcelona, Martí i Franquès 1, 08028 Barcelona, Spain

[§]Consiglio Nazionale delle Ricerche, Istituto di Chimica dei Composti Organometallici (CNR-ICCOM), Via Madonna del Piano 10, 50019 Sesto Fiorentino (FI), Italy

[∥]Department of Biochemistry, Duke University, Durham, North Carolina 27710, United States

[⊥]Department of Chemistry, Carleton University, Ottawa, ON K1S5B6, Canada

Supporting Information

ABSTRACT: We begin with a brief historical review of the development of our understanding of the normal ordering of nd orbitals of a transition metal interacting with ligands, the most common cases being three below two in an octahedral environment, two below three in tetrahedral coordination, and four below one in a square-planar environment. From the molecular orbital construction of these ligand field splittings evolves a strategy for inverting the normal order: the obvious way to achieve this is to raise the ligand levels above the metal d's; that is, make the ligands better Lewis bases. However, things are not so simple, for such metal/ligand level placement may lead to redox processes. For 18-electron octahedral complexes one can create the inverted situation, but it manifests itself in the makeup of valence orbitals (are they mainly on metal or ligands?) rather than energy. One can also see the effect, in small ways, in tetrahedral Zn(II) complexes. We construct several examples of inverted ligand field systems with a hypothetical but not unrealistic $AlCH_3$ ligand and sketch the consequences of inversion on reactivity. Special attention is paid to the square-planar case, exemplified by $[Cu(CF_3)_4]^-$, in which Snyder had the foresight to see a case of an inverted field, with the empty valence orbital being primarily ligand centered, the d_{x2-y2} orbital heavily occupied, in what would normally be called a Cu(III) complex. For $[Cu(CF_3)_4]^-$ we provide theoretical evidence from electron distributions, geometry of the ligands, thermochemistry of molecule formation, and the energetics of abstraction of a CF_3 ligand by a base, all consistent with oxidation of the ligands in this molecule. In $[Cu(CF_3)_4]^-$, and perhaps more complexes on the right side of the transition series than one has imagined, some ligands are σ-noninnocent. Exploration of inverted ligand fields helps us see the continuous, borderless transition from transition metal to main group bonding. We also give voice to a friendly disagreement on oxidation states in these remarkable molecules.

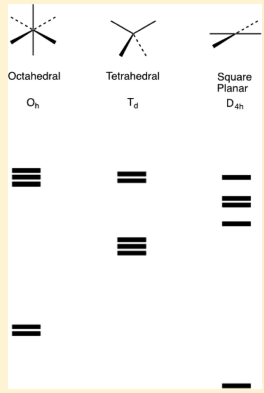

CONTENTS

Received: April 20, 2016
Published: July 11, 2016

DOI: 10.1021/acs.chemrev.6b00251
Chem. Rev. 2016, 116, 8173−8192

1. INTRODUCTION

1.1. History of Crystal and Ligand Field Theory

That the 3d electrons of a transition metal split in an octahedral ligand field, with a triply degenerate level (now labeled by its O_h irreducible representation as t_{2g}) coming below a doubly degenerate e_g level, this was made crystal clear in Hans Bethe's remarkable 1929 paper.[1] A few years later it was reasoned out that in a tetrahedral environment the opposite splitting, e below t_2, occurs.[2] In time, the crystal field approach, basically a sound quantum mechanical, group-theory-informed analysis of the repulsion of the metal atom/ion electrons for electrons borne by what we would now call ligands, was extended by a variety of quantum mechanical approaches: ligand-field theory, the angular overlap model, and simple molecular orbital (MO) theory.[3−8]

Today, the student of inorganic chemistry is likely to come to the classic t_{2g} below e_g splitting of the d levels through a molecular orbital interaction diagram, such as that shown in Figure. 1.[9] We note parenthetically that Clark Landis and Frank Weinhold have argued that np orbitals are unimportant in transition metal chemistry,[10] but this claim has been contested.[11−13]

It is not easy to trace back in the literature the first use of such a diagram. The essential part of it is in the equally classic 1935 paper of John Van Vleck (Figure 2), who for the first time used the contemporary group-theoretical notation but in the diagram shown retains Bethe's labels for ε (t_{2g}) and γ (e_g) levels.[14] With the development of the ferrocene bonding story, the renaissance of crystal field theory in the hands of chemists in the 1950s, the pedagogically effective and influential text of Orgel,[15] and the timely review by Moffitt and Ballhausen,[16] orbital interaction diagrams (like that of Figure 1) became part of every inorganic chemistry course around the world.

There is an implicit assumption in Figure 1, which needs to be spelled out, for it is essential to what will follow: the ligand (Lewis base) orbitals are placed in the interaction diagram in energy below the metal d functions. The consequence is, simplistically, that the e_g set that is pushed up in energy is mainly metal and that the e_g set that goes down is mainly ligand in character. The assumed ligand and metal orbital ordering in energy is a natural one; the ionization potentials of transition metal d orbitals are generally substantially smaller than those of typical Lewis base ligands, be they amines, phosphine, CO, or an ethylene.

Note that the above considerations address only the σ bonding in these molecules; the effects of π-bonding have been long recognized; they can shift the energy of the t_{2g} levels up and down in an understandable manner.

1.2. What Will Be Done in this Paper

So far, we have reviewed the known, what is taught in our courses (perhaps they lack a bit the history). This forms the background for what we will do in this contribution: We will probe our current understanding of bonding in transition metal

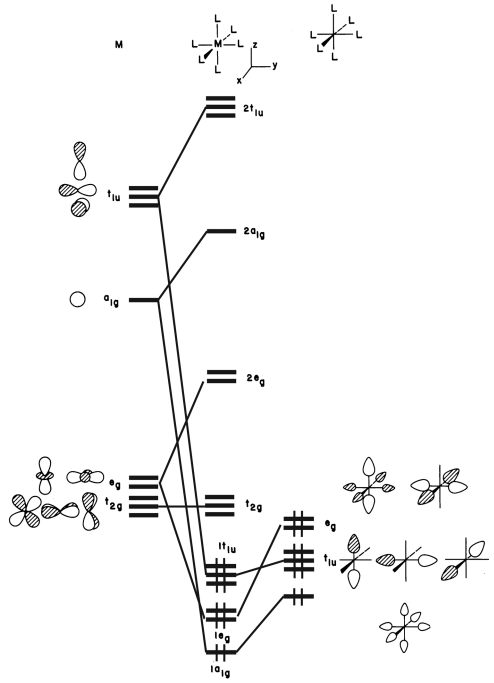

Figure 1. Orbital interaction diagram for a transition metal ion interacting with 6 Lewis base ligands. Reproduced with permission from ref 9. Copyright 2013 John Wiley and Sons. The electron count shown is for a d^0 complex; the more common 18-electron octahedral complexes, such as $Cr(CO)_6$, will have 6 electrons in the t_{2g}. This diagram does not yet take into account the π-bonding capabilities of the ligands.

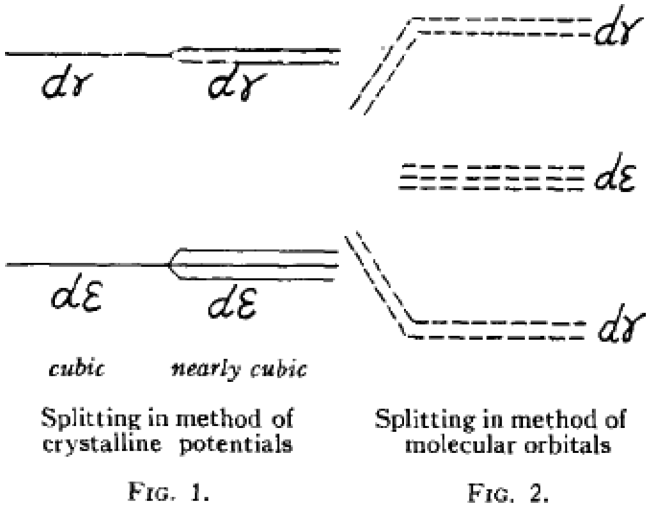

Figure 2. First (perhaps) orbital interaction diagram in a molecular orbital discussion of an octahedral complex. Reproduced with permission from ref 14. Copyright 2013 American Institute of Physics. Note that for Van Vleck (as for most physicists at the time) cubic did not mean 8 ligands at the corners of a cube surrounding the metal, but implied an octahedral environment of the metal ion, one of the cubic point groups.

complexes by turning the received wisdom, oh so useful, on its head: is it conceivable to invert classical ligand field splitting patterns? We will review what is in the literature on the subject, for we did not come to this seemingly outlandish proposition ab initio. Finally, we will review a foresightful analysis 20 years ago, of an unusual anion, $[Cu(CF_3)_4]^-$, by James Snyder. His

DOI: 10.1021/acs.chemrev.6b00251
Chem. Rev. 2016, 116, 8173−8192

suggestion for the bonding in this putative Cu(III) complex, recently experimentally verified, is critical in establishing the existence of ligand field inversion and, eventually, leads us to a unifying perspective that does not dichotomize transition metal and main group compounds (and the bonding in them) but sees them as ends of a continuum.

1.3. Strategy for Inverting Ligand Fields

The three most common ligand environments of a metal ion/atom in coordination, organometallic, and solid state inorganic chemistry are the octahedral one (whose history was worth tracing above), and, additionally, tetrahedral and square-planar coordination. The typical crystal field−ligand-field−molecular orbital splittings in these coordination environments are shown in Figure 3, three below two for the octahedron, two below

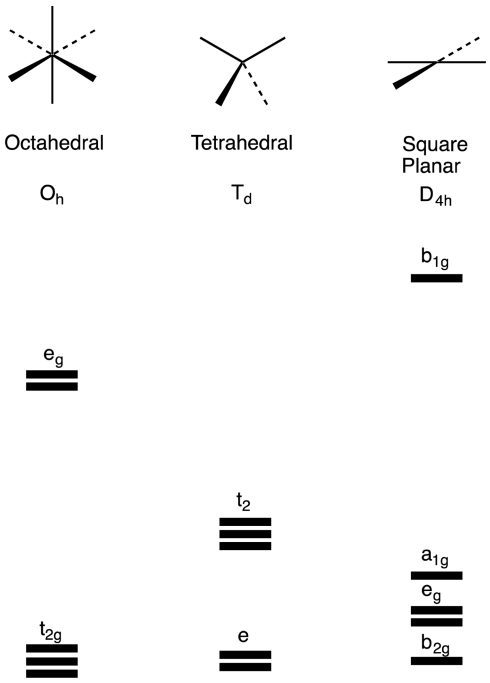

Figure 3. Three most common ligand-field splittings.

three for the tetrahedron (and cube), and four below one for square-planar coordination. From this point on we will refer to these splittings as "normal ligand-field" splittings, fully aware of the distinction between the crystal field, ligand-field and molecular orbital ways of deriving them. Cirera and Alvarez have summarized the ligand field splittings for other coordination numbers and geometries.[17]

Can we invert these three situations, i.e., put two below three in the octahedron, three below two in the tetrahedron, and one below four in the square? That is the subject of this paper.

The obvious solution, suggested by our pointing to the ordering of levels implicit in the "normal" construction, is to look at ligands whose Lewis base donor orbitals are not below the metal nd levels but above them or to vary the metal to accomplish a similar aim. As we will see, things are hardly so simple.

However, first a little history.

1.4. How Three Groups Came to the Problem

The three groups joining in this contribution found pointers to the underlying question in a variety of ways.

The Hoffmann group, engaged in (too) many calculations of molecular complexes and solid state compounds, came along the way upon three unusual computational outcomes:

1. One was in a study of phases that use a simple hexagonal net as a building block, exemplified by the CaCuSi or ZrGeSn structure, Figure 4, top left. In a calculation on a $PtSi^{2-}$ sheet as a model for these compounds, it was noted that the highest energy bands were primarily Si based not on the metal.[18]

2. In a second, very different study of the adsorption of CO on PtBi and $PtBi_2$ surfaces, it was noticed in bulk $PtBi_2$, which featured a Pt ion, formally Pt^{4+}, approximately octahedrally coordinated by Bi_2^{4-} pairs (see Figure 4 bottom left), a rather small ligand-field splitting and primarily Bi-based high-lying bands. A calculation of a molecular $Pt(BiH_3)_6^{4+}$ model gave a splitting of metal d levels where, among the primarily Pt-based levels, the t_{2g} was higher in energy than the e_g.[19] The "inverse ligand field" was traced to a position of ligand levels (Bi based) above the metal d orbitals.

3. The third case was brought to us by Wojciech Grochala. Ag(II) and Ag (III) are among the most oxidizing oxidation states known; they even oxidize, or come close to doing so, the fluoride ion to F, i.e., F_2. Ag(II) complexes cannot be handled in solution because they oxidize water. Figure 4, right, shows the structure of one of the few known well-characterized Ag(III) salts, $KAgF_4$. In calculations on this salt, as well as other Ag(II) and Ag(III) compounds, we found that the Ag d orbitals were actually below the (very low-lying) fluoride ligand orbitals.[20] Grochala, who was the driving force in the above work, has independently continued to seek out examples of inverted ligand-field splittings.[21,22] Also, using Ag and F core and valence spectroscopies, Grochala and co-workers have shown that in $KAgF_4$ the Ag 4d orbitals are below the fluoride levels. To use their words, that in the putative Ag[III] complex "one sees the intrinsic property of holes being introduced in F(2p) band".[23] We will see the like in the electronic structure of $[Cu(CF_3)_4]^-$.

The Mealli group early on developed a program, CACAO,[24] which afforded visual MO analyses based on perturbation theory principles.[25] When applied to inorganic molecules, the common idea of L → M dative bonding generally fit what was observed, but occasionally the gap between metal and ligand orbitals was small; the orbital energy order even reversed. This result occurred with a quite electronegative metal (e.g., Ni or Cu) bound to an electropositive ligand atom such as B, Si, or Sn. In this case, a higher fraction of the bonding electrons could be attributed to the metal, suggesting an inverted M → L dative bond or σ-backdonation.[26] To be specific:

4. The first case noticed was the Ni−Sn linkage in the trigonal bipyramidal (TBP) complex $[(np_3)Ni(SnR_3)]^+$, where np_3 is the tetradentate tripod $N(CH_2CH_2PPh_2)_3$.[27] Support for the idea was provided by the chemistry of the immediate precursor $(np_3)Ni$, which exists independently, and may add the SnR_3^+ cation without changing the zero oxidation state of the metal. In fact, the electronegativity of the metal is such that the z^2 axial lone pair does not substantially transfer electrons to form a stannyl anion and the corresponding Ni(II). The system is best described as an SnR_3^+ adduct. Others later pointed out a similar picture, for comparable cases.[28]

5. The inverted ligand field concept applies even better for a metal simultaneously bound to two or more electropositive atoms (e.g., several cases of a Pd center bonded with up to six silyl groups are known). Due to the proximity of the ligands to each other, especially for higher coordination numbers,

DOI: 10.1021/acs.chemrev.6b00251
Chem. Rev. 2016, 116, 8173−8192

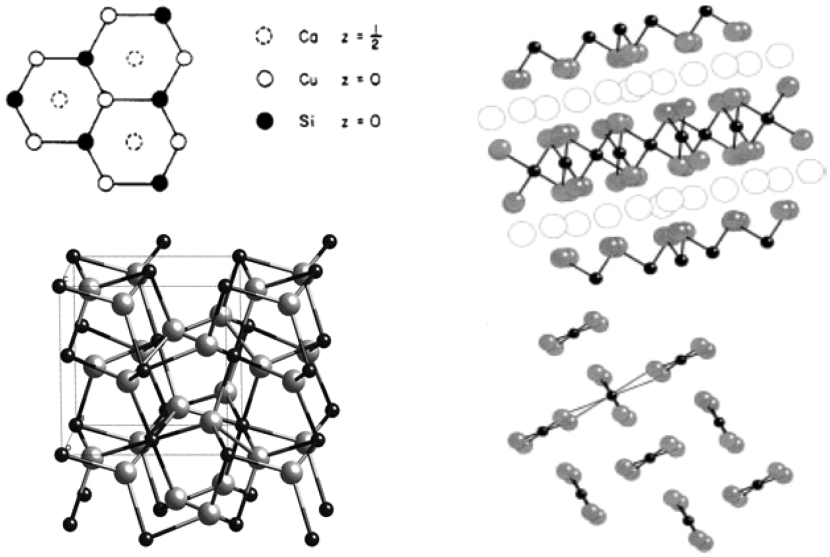

Figure 4. (left, top) Segment of the CaCuSi structure; (left, bottom) one view of the bulk $PtBi_2$ structure; note Bi_2 pairs and approximately octahedral coordination of the Pt ions; (right) crystal structure of $KAgF_4$; a view showing the layers of isolated square $[AgF_4]^-$ ions (right, top); Ag: black spheres, K: white spheres, F: gray spheres; a view showing the relative orientation of the square $[AgF_4]^-$ ions (right, bottom).

antibonding ligand σ hybrid combinations may rise in energy substantially above metal orbitals. So the donor−acceptor relationship in a complex may be influenced by geometry as well.

The effect of the geometry clearly emerged from an early qualitative analysis[29] of pseudo-octahedral Co(III) complexes as models of vitamin B_{12}.[30] In nature, this vital system consists of a tetradentate and equatorial corrin ring associated with coaxial Co-CR_3 and Co−$N_{imidazole}$ linkages. Several biomimetic models were derived, starting from a square planar Co(I) complex to which an alkyl halide and a nitrogen base were added. As for the SnR_3^+ adduct, the filled z^2 orbital of the metal is potentially available for an inner sphere redox process. The collinear N base was noticed to play an important role; until the base is separated or weakly bound to the metal, z^2 is scarcely affected. On shortening the Co−N distance, z^2 is pushed higher in energy; the reduced gap with the CR_3^+ σ hybrid can eventually favor the inner transfer of two electrons from the Co(I) ion to carbon. For an intermediate Co−N distance of about 2.4 Å, it was observed that the Co−C σ and σ^* levels are only slightly separated and a triplet is accessible. A fragmentation to a five-coordinated Co(II) fragment and a methyl radical then becomes possible,[29] consistent with the radical reactivity in the biological substrate.[31]

6. Another example of what could be called essential σ-backdonation was noticed by Mealli in calculations on dimers of formula Cp′(Ru)(μ-H)$_4$RuCp′[32] with four putative hydride bridges and formal Ru(III) ions. An early theoretical analysis attributed the short Ru−Ru distance of ∼2.46 Å to four combined $2e^-/3c$ bonds.[33] However, a combination of out-of-phase H s orbitals (b_{1g}) is already much destabilized in energy and this MO can uniquely interact with a lower in-phase combination of d_δ orbitals (see Figure 5).

In this system, it makes more sense to consider one bridging H as positive. The metal oxidation state then has two Ru(II) rather than Ru(III) ions. The viewpoint is consistent with the full population of the "t_{2g}"-like levels, as one sees in any calculation.[34]

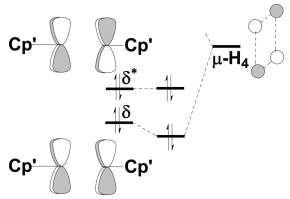

Figure 5. Molecular orbital interaction diagram showing the high energy b_{1g} H combination interacting with an occupied cyclopentadienyl orbital.

The Alvarez group came to inverted ligand field considerations through the following problems:

7. The band structure of $MoNiP_8$ calculated by them[35] was inconsistent with a classical electron counting scheme, in which the charge of P_8^{6-} groups would require the metal oxidation states Mo^{4+} and Ni^{2+}. Instead, the e_g-type orbitals of the octahedrally coordinated nickel atom were found to be the major components of an occupied band below the t_{2g} one, in a clear inverted ligand field splitting. Consistently, the bands around the Fermi level, including Ni−P antibonding orbitals, were mainly phosphorus in character.

8. Another study, by Alvarez and co-workers, of a solid state phosphide, CoP_3, a paradigmatic example of the wide family of skutterudites,[36,37] revealed also the e_g band of the octahedral cobalt atoms at lower energy than the t_{2g} one (Figure 6).

The skutterudite CoP_3 structure can be considered as derived from the more symmetric ReO_3 one, by approaching the phosphide ions of a hypothetical $Co^{IX}(P^{3-})_3$ compound with the rhenium trioxide structure, in such a way that they form P_4^{4-} rings and reduce the metal atoms to their Co^{III} oxidation state. Such a process is schematically represented at the orbital level in Figure 6, where the final step consists of the interaction of the high lying π nonbonding and π^* orbitals of the P_4 ring with the metal d-e_g orbitals pushing them below the t_{2g} set and resulting in a formal d^{10} electron configuration for Co. The outcome of the inverted ligand field is that the electrical conductivity in skutterudites seems to be associated with the chains of phosphorus rings rather than the metal atoms.

DOI: 10.1021/acs.chemrev.6b00251
Chem. Rev. 2016, 116, 8173−8192

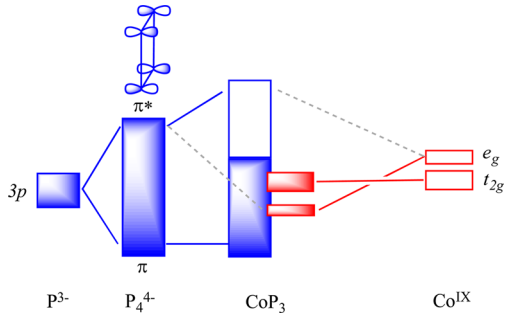

Figure 6. Interaction of the occupied p band of the sublattice of P_4^{4-} rings with the Co d block bands in CoP_3.

The conversion of ReO_3 itself to a skutterudite structure was shown to be unfavorable because the O−O antibonding levels fall below the metal ones, due to the higher O electronegativity. Thus, in the case of CoP_3, both the low electronegativity of phosphorus and the formation of P−P bonds, akin to reductive elimination reactions in organometallic chemistry, seem to favor the inverted ligand field. In contrast to organometallic reductive elimination, though, here the P−P bonds formed remain attached to the metal atoms and do not dissociate due to the existence of further bonding capability at these atoms.

As one can see, there were many ways in to the question. In a published trialogue, the three groups debated the possible bonding between the two S capping atoms of a Cu_3 compound. Possible inversion of the ligand field also figured there.[38]

Inversions of normal ligand fields have also come up in the work of others. For instance, the Peters group has made a series of interesting low-spin, axially distorted pseudotetrahedral Co(II) and Fe(II) complexes for which a three below two level splitting was established.[39−41]

1.5. The Snyder Imbroglio

In 1995 James Snyder published a fascinating theoretical paper[42] on the $[Cu(CF_3)_4]^-$ anion, made in several salts by Naumann et al.[43] A new synthesis from the Grushin group has made this species quite accessible.[44]

Snyder noted a one below four splitting of primarily metal levels in his calculations; that is, the empty level was primarily a ligand-based combination, with just a little metal d_{x2-y2} character (see Figure. 7). He proposed that the formal Cu(III) complex was really Cu(I), with oxidation of the perfluoromethyl ligand set.

Snyder's views were roundly criticized in a subsequent comment by Kaupp and von Schnering,[45] to which Snyder responded.[46] One had to wait for the analysis of Aullón and Alvarez to begin to understand what was really going on in this fascinating system.[47] In recent work from the group of Lancaster,[48] there is new experimental information about this molecule, supporting Snyder's position. We will return to its theoretical analysis below, sorting out, as best as we can the complexities of oxidation state assignment in this molecule and others like it.

We note that ligand field inversion has been proven spectroscopically and discussed, tracing it to the position of the levels of the ligands relative to the metal, as we do, in another case of a square-planar, seemingly Cu(III) complex, one that turns out to be Cu(II).[49] These are the $L_2[Cu_2(S_2)_n]^{2+}$ complexes of York, Brown, and Tolman.[50]

We proceed to describe several attempts to create computationally an inverse ligand field, i.e., to realize the inverse of the

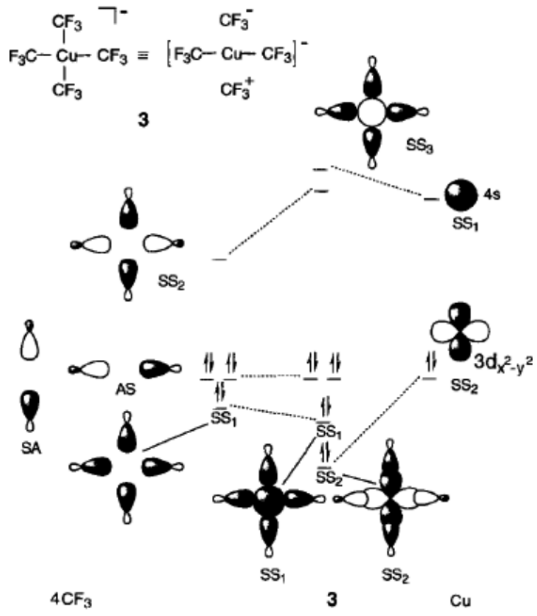

Figure 7. Snyder's interaction diagram for $[Cu(CF_3)_4]^-$. Reproduced with permission from ref 42. Copyright 1995 Wiley-VCH Verlag GmbH & Co. KGaA.

level situation shown in Figure 3. As we hinted, things are not going to be as simple as some of us had thought.

2. COMPUTATIONAL PROBING OF THE POSSIBILITY OF INVERTING LIGAND FIELDS

2.1. Using the Strength (=Weakness) of Extended Hückel Calculations to Get Oriented

We thought it is instructive to do a calculation on an octahedral 18-electron ML_6 and tune the donor ability of the ligands. Octahedral $[MH_6]^{q-}$ anions are known in extended structures,[51−59] and there are calculations of these, for instance for Y_2CrH_6.[60] However, normal quantum chemistry calculations are probably not the way to approach the tuning we wish to effect. A calculation on isolated $[CrH_6]^{6-}$, unlikely to converge in a normal density functional theory (DFT) calculation, is no problem for the extended Hückel (eH) procedure,[61] for in applying it one does not (usually) make its parameters depend on charge. A weakness, to be sure, for the energy levels of real molecules respond dramatically to charge on the molecule, but also a strength of eH, for it allows one to study trends that are not easily approached by the better calculations.

To see the effect of the energy of the ligand orbitals on the ligand-field splitting, we simply tuned the H_{ii}, the diagonal matrix element or Coulomb integral of the hydride ligands (see SI) in extended Hückel calculations performed with the CACAO program of Mealli, Proserpio, and Ienco.[24] Comparative interaction diagrams are shown in the upper part of Table 1. The six O_h symmetry combinations of hydrogens (a_{1g}, e_g and t_{1u}) at both the left and right sides are for different H_{ii} values of −13.6 and −8.6 eV, respectively.[62] The slight splitting of the hydride ligands is due to the small overlap with each other. For the realistic −13.6 eV H orbital energy, all the H combinations lie below the metal orbital, consistent with the medium donor character of the ligand. For a more negative H_{ii} value, they would lie still lower, their donor power weakened.

The filled t_{2g} metal level remains at the assumed Cr value of −11.2 eV, unperturbed and pure metal for the lack of π−

DOI: 10.1021/acs.chemrev.6b00251
Chem. Rev. 2016, 116, 8173−8192

Table 1. Comparative eH Interaction Diagrams for the Formation of O_h $[CrH_6]^{6-}$ with different H_{ii} Values (in eV) for the H Ligands

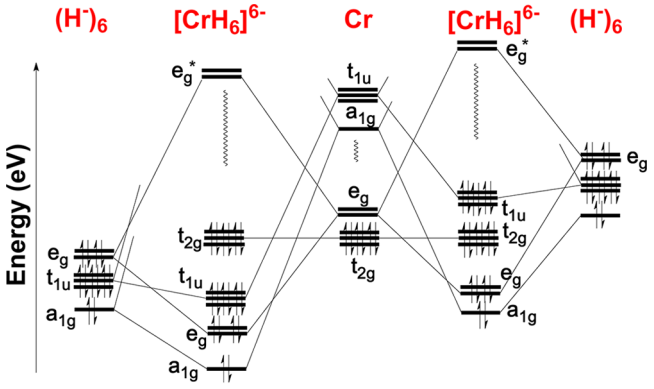

$(H_{ii}$=-13.6)

O_h	En.(eV)	Cr%	H_6%
e_g*	-1.2	55	45
t_{2g}	-11.2	100	0
t_{1u}	-14.3	21	79
e_g	-14.7	45	55
a_{1g}	-16 .9	23	77

$(H_{ii}$=-8.6)

O_h	En.(eV)	Cr%	H_6%
e_g*	-1.2	22	78
t_{1u}	-9.6	33	67
t_{2g}	-11.2	100	0
e_g	-12.2	78	22
a_{1g}	-12.5	44	56

bonding capabilities at the H ligands. In each case, there is a filled e_g level, and an unfilled one, both with d_{x2-y2} and d_{z2} metal participation. The character of the resulting e_g MOs is strictly dependent on the energy of the ligand orbitals. Thus, on changing the H potential from −13.6 to −8.6 eV, the antibonding e_g* level clearly inverts its composition (see Table 1). From 55% metal character for H_{ii} = −13.6 eV, it becomes 78% ligand at −8.6 eV. Exactly the opposite happens for the bonding e_g counterpart, which loses its typical L → M dative character, to become 78% metal centered.

It becomes obvious that the initial strategy of creating an "inverted" ligand field was not well thought through. One can, of course, make the ligands better donors, higher in the energy of their Lewis base orbitals than the metal nd. This is modeled theoretically by H_{ii} tuning, and in reality may be achieved by anionic charge on the ligands or by moving down group 14, 15, and 16 (more of this in time) or over to group 13. No matter what one does, there are (neglecting π bonding) two sets of e_g orbitals, and only one is filled. What changes with ligand donor capability is the composition of the two e_g orbital sets; if the donors are "normal" or relatively poor, the occupied e_g orbitals are more localized on the ligands, and if the donors are supergood, the occupied e_g set is more on the metals.

To put it another way, the movement of the donor orbitals to higher energy achieves an inverse ligand field, in that in the primarily metal orbitals e_g comes below t_{2g}. However, identifying that this is so is not going to be easy.

2.2. Telling the Composition of Orbitals

The techniques for identifying the composition of orbitals (are they mainly on the metal or on the ligands?) are not many. One general group of techniques are X-ray, or core spectroscopies, where transitions involve electronic excitation from or demotion to core orbitals. Excitation and emission energies are widely separated between elements; consequently, these methods allow one to to explore individual transition metal centers in any milieu.

Typically, K-edge (1s → valence/continuum) X-ray absorption spectroscopy (XAS) has been used to elucidate the "physical" oxidation states of transition metals, although competing effects on "rising edge" positions can confound assignments. However, the usual dipole selection rules can be leveraged through core spectroscopies, in which an electron is excited from a core level, and one observes transitions to fill the resultant hole. Since the initial excitation is very atom-specific, the selection rules in principle will give greater intensity to compensating cascades according to the contribution of the excited atom to the levels.

Given the usual dipole selection rules, a combination of K and L (2s/2p → valence/continuum) edge measurements can provide detailed experimental information on the composition of molecular orbitals.[63] Resonant inelastic X-ray scattering (RIXS) and XAS have, for instance, been applied in this way to the study of bonding in $Fe(CO)_5$.[64] Ligand field inversion was demonstrated by such techniques (combining Cu K- and L-edge with S K-edge XAS), as we have mentioned, for what might have been thought as a square-planar Cu(III) complex, but in fact emerges as Cu(II).[49] We will have occasion to cite an exemplary study applying just such techniques, in the context of precisely the $[Cu(CF_3)_4]^-$ ion, from the Lancaster group.[48]

Information might also be obtained from electronic spectra. The excitation of transition metal complexes can be classified as d-to-d, metal to metal, generally weak as they are dipole-forbidden, and metal to ligand or ligand to metal excitations, of a charge transfer nature, are potentially strong. Different orbital compositions (for instance e_g and e_g* in the octahedral case discussed) may affect substantially the intensity of such transitions.

2.3. If There Is an Inverted Ligand Field, Is the Metal Perforce Reduced?

Oxidation states are a convenient fiction, yet immensely useful in chemistry.[65−68] Quantum mechanics is not going to be of much help in defining these; just the fact that there are Mulliken, Wiberg, Bader, and Mayer charges in the literature tells you that any partition of electrons in a molecule among atoms may be uniquely defined but ultimately will be arbitrary. Experimental "measurements" of charges are also best taken with a large grain of salt; theoretical manipulation of the observables is always involved. It is still possible, as Aullón and Alvarez showed,[47] to find a chemically sound way of differentiating oxidation states in calculations.

The reason for our minor tirade on oxidation states is that the quest for an inverted ligand field inevitably gets involved with questions of oxidation and reduction. As follows:

1. You will notice that in Figure 1, the "normal" case, the 12 electrons of the six Lewis base ligands move to lower energy upon interaction, and the six valence electrons of the metal (if it were Cr, Mo, and W) would enter the t_{2g} orbital, resulting in a low-spin 18-electron complex. However, what if the ligand levels were above in energy, sometimes way above, the metal levels, which is where they would be for a supergood donor? Would not one then have a better starting point for thinking about electron flow and bonding in such cases by first transferring some electrons to the metal, i.e., reducing it? This perspective informed Snyder's reasoning in the $[Cu(CF_3)_4]^-$ case.

So, could it be that it is better to speak of oxidation/reduction of ligands/metals than of an inverse ligand field? We

DOI: 10.1021/acs.chemrev.6b00251
Chem. Rev. 2016, 116, 8173−8192

will return to this question, and provide some chemical consequences.

2. To quote Ecclesiastes 1:9, there is nothing new under the sun. $Fe(CO)_4H_2$ is a known molecule, whose experimental structure[69,70] is presented in Figure 8.[71] Is it a distorted (for

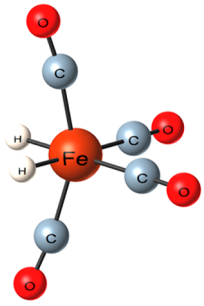

Figure 8. Structure of $Fe(CO)_4H_2$ as determined from gas phase diffraction (ref 69).

steric reasons) d^6 octahedral complex of Fe(II)? Or is it a diprotonated d^{10} $[Fe(CO)_4]^{2-}$, basically tetrahedral, but deformed, perhaps for steric reasons, following face-protonation (where there are maxima of electron density) of the expected tetrahedral dianion? The FeC_4 group in $Fe(CO)_4H_2$ is, in terms of continuous shape measures,[72,73] 65% along the minimal distortion pathway from a tetrahedron to a cis-divacant octahedron.

Both viewpoints have validity and connect up to much other chemistry, of octahedral d^6 six-coordinated complexes and of tetrahedral four-coordinated d^{10} ones. We can also think of this molecule as being a case of an inverted ligand field.

The inherent ambiguity in assigning oxidation states in organometallic chemistry surfaced early on, as a reviewer reminded us, in the considerations of the bonding in olefin complexes: are they such or metallacyclopropanes?[74−76] The reader is also directed to a thoughtful discussion of donor and acceptor perspectives in inorganic chemistry by Mingos.[77,78] We also mention here an interesting resent paper by Goesten and co-workers, on six-coordinated group 13 complexes.[79] They argue convincingly that the bonding in these should be seen as electron-rich hypervalent. One can also see the remnants of an inverted ligand field in their orbitals. As we move from left to right in the periodic table, the d orbitals go deeper, become core-like in late transition metals and the Zn group, and core in the p-block, leading to hypervalency. There is a continuous path from normal ligand field to inverted ligand field to hypervalence.

2.4. Can It Happen in a Tetrahedron?

To return to efforts to create or observe an inverted ligand field, we thought we might reduce the ambiguities of octahedral coordination, where the ligand-field destabilized orbital was unfilled, by moving to a tetrahedral d^{10} complex. The classical (normal) molecular orbital diagram is shown in Figure 9.

Our initial idea was to probe the tuning of donor capability with $[Ni(EH_3)_4]$, E = N, P, As, Sb, and Bi, so as to avoid complications with ligand π-bonding as one might have in the carbonyls. We also wished to move beyond extended Hückel calculations.

Well, "The best-laid schemes o' mice an' men gang aft agley."[80] Our struggles to find a model system have been relegated to the Supporting Information (SI) of this paper.

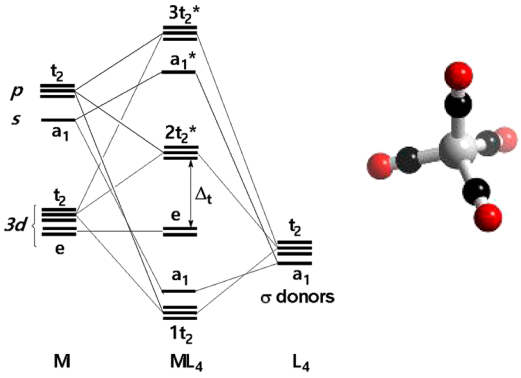

Figure 9. (left) Molecular orbital construction of the valence orbitals of a tetrahedral complex; (right) $Ni(CO)_4$.

Briefly, we had forgotten the potential instability of many d^{10} ML_4 complexes[81,82] and that the decomposition to a stable d^{10} ML_2 and free ligands looms as an energetic alternative.[83,84] This is what calculations indicate for all ammine complexes. If we now move away from E = N, all $M(EH_3)_4$ T_d structures for M = Ni, Pd, and Pt and E = P, As, Sb, and Bi are found to be local minima. Unfortunately, we still cannot tune the donor capability of EH_3 simply based on the electronegativity of E. For instance, BiH_3 is found to be a worse donor than PH_3. The energy of the BiH_3 lone pair is below that of PH_3, and its overlap with a model acceptor (taken as BH_3), smaller, as gaged by the size of the Fock matrix element between donor and acceptor orbitals. The reason for both phenomena is the much greater ns (vs np) character in the BiH_3 lone pair, a manifestation of the inert electron pair effect of the Bi 6s orbital.[85]

An alternative is to tune the acceptor capability of the metal, i.e., compare $M(EH_3)_4$ given the same E while varying M. We tried this with Ni and Pt, but the realities of the orbital energy ordering did not lead to a clear result. In desperation, we turned to a post-transition metal system, Zn in oxidation state II.

Calculations were carried out on $[Zn(PH_3)_4]^{2+}$ and also on the tetrahalides, $[ZnX_4]^{2-}$, X = F, Cl, Br, and I. The theoretical methodology is described in the SI; briefly the three groups in this work tried consistently to use B3LYP with the SDD pseudopotential and basis set for Cu, Zn, and I and TZVP basis set for the other atomic species. However, in this part, the M06 functional, with an aug-cc-pVTZ (acct) basis set, was used.[86−89] The results are shown in Table 2.We note that the seemingly simpler $[Zn(NH_3)_4]^{2+}$ presents anomalous orbital mixing

Table 2. Energies and Percentage Occupations on Zn and F of the Highest Lying Occupied Orbitals of the Relevant Symmetry shown in Figure for ZnF_4^{2-} and also the Corresponding Orbitals for $[Zn(PH_3)_4](BF_4)_2$

	$[ZnF_4]^{2-}$			$[Zn(PH_3)_4](BF_4)_2$		
orbital	energy/eV	Zn%	F%	energy/eV	Zn%	L%[a]
t_2	0.87	16	84	−11.03−11.12[b]	8	92
a_1	−1.70	19	81	−14.13	46	54
e	−2.86	92	8	−17.73	99	1
t_2	−3.14	82	18	−17.79	96	4

[a]"L" here stands for ligands, including PH_3 and BF_4. [b]Our hypothetical $[Zn(PH_3)_4](BF_4)_2$ structure is of D_{2d} symmetry and the t_2 irreducible representation of T_d correlates to b_2 and e. The degeneracy is correspondingly split.

DOI: 10.1021/acs.chemrev.6b00251
Chem. Rev. 2016, 116, 8173−8192

between the metal d and the ligand's π-like NH bonding orbitals, which is discussed elsewhere.[90] As expected, the net charge on these complexes shifts the orbital energies violently, up in the anions, down in the cations. So the Zn d orbitals were at around −3 eV in the dianions and around −25.5 eV in the dications. We can mitigate the effect by including a counterion in the calculation, for instance computing $[Zn(PH_3)_4](BF_4)_2$. This we did for the dication but not for the tetrahalides. The results, energies and composition of frontier MOs from Mulliken atomic populations, are shown in Table 2. Of the tetrahalides, only $[ZnF_4]^{2-}$ is presented here, the other tetrahalides are in the SI. No imaginary frequencies were found for this anion in its T_d optimized structure, as expected. $[ZnF_4]^{2-}$ is a known complex, in Ca and Sr salts.[91] With the most electronegative F's as the ligands, this species seems unlikely to present us with an example of an inverted ligand field. Yet it does, surprisingly; the Zn contribution dominates in the lower t_2 (82%) and the F contributes more in the higher (84%). Although F is way more electronegative than Zn, with their respective −1 and +2 formal charges, the F^- actually has a higher ligand orbital energy (less electronegative) than the Zn^{2+} 3d, giving the anormalous 2 over 3 d energy order in the tetrahedral metal center. This anomaly is a good manifestation of how charge affects electronegativity. Recall also our mention above of the Ag and F level ordering in $KAgF_4$.[20−23]

To think of it in another way, the d orbitals at the end of the transition series (Cu and Zn) become core-like because of the increasing effective nuclear charge. Once you consider them as core orbitals, it is obvious that the ligands' valence orbitals should be higher in energy and can impart some bonding character to the t_2 set (i.e., push the metal orbitals down in energy, inverting the ligand field). The trend in ns, np, and (n − 1)d level energies with Z is hardly new;[92,93] the connection to ligand field inversion may be. We will return to this observation below.

For $[Zn(PH_3)_4](BF_4)_2$ we ran into unexpected difficulties when we optimized its geometry; the $Zn(PH_3)_4$ part of the molecule moved away from tetrahedral geometry as the BF_4^- units coordinated. The effect will be discussed elsewhere; what is shown in Table 2 is the partitions of critical orbitals for a hypothetical $[Zn(PH_3)_4](BF_4)_2$ structure. It contains a tetrahedral $[Zn(PH_3)_4]^{2+}$, and the two BF_4^- ions are placed on the opposite sides of the S_4 axis of the tetrahedron (see SI for the coordinates). The B atoms are 5 Å away from Zn. Since the Zn 3d orbitals are semicore orbitals, they dominate (96%) in the lower-lying t_2 orbitals. The higher t_2 contains only 8% Zn contribution. One observes a smaller magnitude inverted ligand field compared to $[ZnF_4]^{2-}$, as the orbital mixings in $[Zn(PH_3)_4]^{2+}$ are even milder.

The d^{10} systems considered are certainly not interesting in terms of the d-d electron transition. However, the inverting ligand field has its chance to exhibit itself. For a valence-to-core transition after a core ionization of $[ZnF_4]^{2-}$, the bonding metal-rich t_2 orbital will lose an electron, resulting in longer Zn−F bonds. If it were a normal ligand field, the valence-to-core transition would deplete an antibonding t_2 orbital and shortens the bonds.

We will return to another Zn complex in time.

3. $AlCH_3$ COMPLEXES, EXAMPLES OF INVERTED LIGAND FIELDS

Searching for a two-electron donor atom with a low electronegativity that could facilitate the inverse ligand field situation, we came across a series of ECR_3 ligands, where E is a group 13 element. Apparently the first reported structure of a complex with one such ligand is that of $[Ni(InC\{SiMe_3\}_3)_4]$,[94] which was prepared later with a different degree of solvation.[95] Other tetrahedral complexes with Ga and In donors have also been reported: $[Ni(GaC\{SiMe_3\}_3)_4]$,[2] $[Pt(GaC\{SiMe_3\}_3)_2(dCype)]$,[96] and $[Pt(InC\{SiMe_3\}_3)_4]$.[97] Ligands of that family are also present in mixed ligand complexes with octahedral geometry or with higher coordination numbers: $[Mo(Ga\{\eta^1\text{-}Cp^*\})\ (Ga\{\eta^5\text{-}Cp^*\})_5]$,[98] $[Mo(GaMe)_2(ZnMe)_4.(Zn\{\eta^5\text{-}Cp^*\})_4]$,[99] $[Ru(InC\{SiMe_3\}_3)_3Cp^*]^+$,[100] $[Rh(GaMe)(Ga\{\eta^5\text{-}Cp^*\})_4]^+$,[101] $[Ru(Ga\{\eta^1\text{-}Cp^*\})_3(Ga\{\eta^5\text{-}Cp^*\})_3][Ru(Ga\{\eta^1\text{-}Cp^*\})_4(\{\eta^5\text{-}Cp^*\})_2]$,[102] $[Rh(In\{\eta^1\text{-}Cp^*\})\ (In\{C_5Me_5\}\text{-}InCp^*]$,[103] $[Mo(GaMe)_4(ZnCp^*)_4]$,[98,99] and $[Rh(GaMe)(ZnMe)_3(ZnCp^*)_4]$.[99] Computational studies on the compounds of general formula $[Ni(EMe)_4]$ were reported by Uhl et al., who showed these ligands to be strong π-acceptors.[95]

We have carried out a geometry optimization on the hypothetical complex $[Rh(AlMe)_4]^+$, which could be described formally as a rhodium(I) compound with neutral two-electron σ-donor and π-acceptor AlMe ligands. The reason we moved from the known tetrahedral, formally d^{10} complexes to a formally d^8 model is that we wanted to set up an analogy to the $[Cu(CF_3)_4]^-$ case. The energy minimum presents a slightly pyramidalized geometry, as shown in Figure 10.

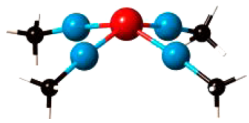

Figure 10. Optimized geometry of $[Rh(AlMe)_4]^+$. Color code: Rh, red; Al, blue; C, black; H, white.

The Mulliken charges in this complex are −0.67 and +0.52 for the Rh and each of the Al atoms, respectively. The analysis of the molecular orbitals in the planar form is shown in Figure 11. There we can see that the negative charge at the rhodium atom is just the outcome of the inverse ligand field. Indeed, if we focus on the b_{1g} MOs (although actually b_1 in the optimized C_{4v} symmetry, we use the D_{4h} symmetry labels for simplicity), we find an occupied x^2-y^2 orbital at the bottom of the d-block (47% x^2-y^2 contribution), while the empty b_{1g} counterpart is mostly centered at the Al atoms (18% Rh x^2-y^2 and 78% Al contribution). In fact the Rh x^2-y^2 orbital is so stabilized that it is distributed among two occupied MOs that mix Rh−Al and Al−C bonding, adding up to an 80% contribution of the rhodium d orbital.

A result of the loss of planarity of the molecule is that the xz and yz orbitals strongly mix with the metal's p_x and p_y, adding Rh−Al σ character to the corresponding MOs. As a consequence, there is extensive mixing of three occupied e_u MOs that incorporate xz and yz contributions, together with Rh−Al bonding and C−Al bonding character. While the appearance of the x^2-y^2, xz and yz metal orbitals in two occupied molecular orbitals each can be easily understood as a delocalized version of the corresponding C−Al and Al−Rh bonding orbitals (illustrated schematically in Figure 12, left for the case of x^2-y^2), the outward hybridization of the e_g couple (xz and yz) assures significant lone-pair character in these two MOs (Figure 12, right). Taking into account the four Al atoms and the two lone pairs, one could describe a trigonal prismatic coordination geometry around the Rh atom.

DOI: 10.1021/acs.chemrev.6b00251
Chem. Rev. 2016, 116, 8173−8192

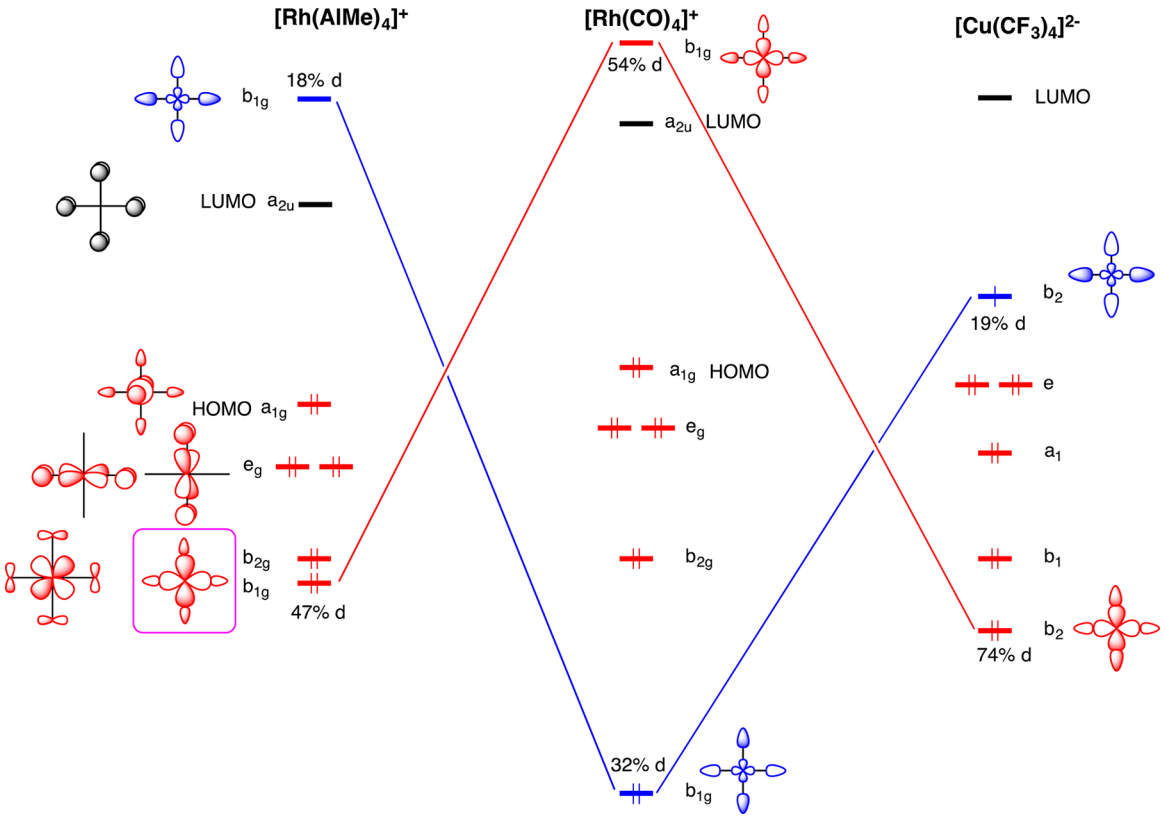

Figure 11. Idealized representation of the molecular orbitals of $[Rh(AlMe)_4]^+$ with significant participation of the metal d atomic orbitals (left), compared to the corresponding orbital diagrams for $[Rh(CO)_4]^+$ (center) and $[Cu(CF_3)_4]^{2-}$ (right). Ligand centered orbitals in blue, transition metal centered orbitals in red. The orbital compositions come from a Mulliken population analysis.

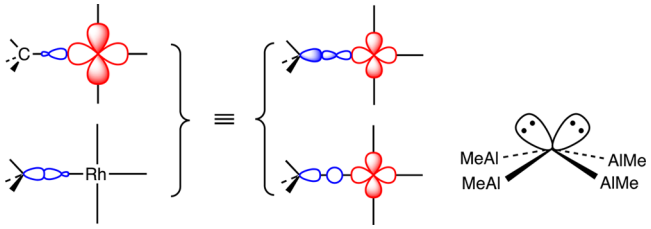

Figure 12. (left) Localized and delocalized pictures of Rh−Al−C bonding in $[Rh(AlMe)_4]^+$; (right) schematic lone pair character in $[Rh(AlMe)_4]^+$.

Both the orbital and the population analyses point to a description of this complex with an effective oxidation state Rh(-I) and two positive charges delocalized throughout the four Al atoms, similarly to what was proposed by Snyder for $[Cu(CF_3)_4]^-$. Note that, in contrast to the copper case, here the metal atom is no longer square-planar.

It is instructive to compare the MO diagram at left in Figure 11 with that for a "classical" square planar rhodium complex, that of the $[Rh(CO)_4]^+$ cation (middle of Figure 11), and notice specifically the very different composition of the bonding and antibonding versions of the x^2-y^2 (b_{1g}) orbital. It is also instructive to compare with the MOs of $[Cu(CF_3)_4]^{2-}$, for which the singly occupied MO has a small (19%) x^2-y^2 contribution, but still a little higher than the contribution from an individual CF_3 group (17%). When added up, the four C atoms carry 67% of the unpaired electron.

The complexities of these fascinating AlMe complexes are not fully described by this analysis. The potential repulsive interaction between the filled d-block and the Al donor lone pairs appears to be mitigated; one needs to analyze the extent of metal s and p participation. There is substantial Al−Al interaction, as gaged by an overlap population 2/3 that of the Al−C bonds. A fragment MO analysis suggests back-donation from metal xy to an appropriate symmetry in-plane bonding combination of Al p orbitals.

Will one see the same effect in a six-coordinated homoleptic complex of AlMe? As a model with a formal d^6 electron configuration we have chosen $[Mo(AlMe)_6]$. Geometry optimization of such a molecule results in a trigonal prismatic structure (Figure 13), an unusual stereochemistry for a d^6 complex.[104] The occupied molecular orbitals with Mo d contributions appear to be metal centered in the case of the e″ (xz and yz) and a'_1 (z^2) orbitals (Figure 14). The e′ set (xy and x^2-y^2) appears shared between two occupied MOs, with intensive mixing into the Al−C π bonding orbitals of the same symmetry, and their total contributions to the two e′ sets

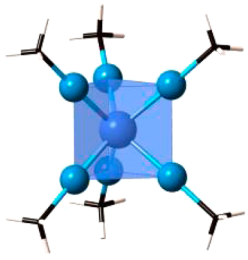

Figure 13. Optimized geometry of $[Mo(AlMe)_6]$. Color code: blue, central Mo and Al; black, C; white, H.

DOI: 10.1021/acs.chemrev.6b00251
Chem. Rev. 2016, 116, 8173−8192

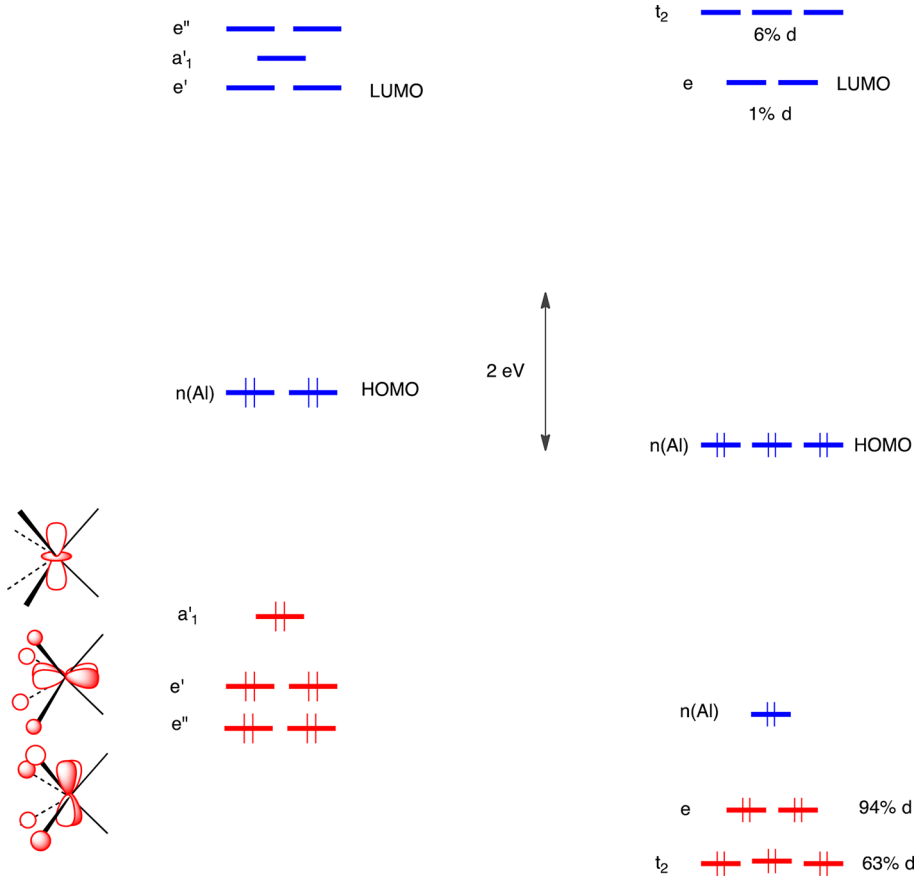

Figure 14. Relevant molecular orbitals of trigonal prismatic $[Mo(AlMe)_6]$ (left) and tetrahedral $[Pd(AlMe)_4]$ (right). Metal d orbitals in red; Al orbitals in blue.

represent a 57% of d character from each xy and x^2-y^2. Moreover, it is seen that the e″ d-MOs have metal−ligand bonding character and are stabilized below the formally nonbonding a'_1 (z^2). The resulting splitting pattern (a'_1 > e′ > e″) is therefore inverted from that found in classical trigonal prismatic complexes (a'_1 < e′ < e″).[17] Given the composition of the occupied orbitals, one might formally ascribe a d^{10} electron configuration and a formal oxidation state of −4 to the Mo atom, whose d^{10} configuration is consistent with the trigonal prismatic geometry found. The −4 oxidation state, however, is not supported by the Mulliken atomic charge, which is negative but much smaller (−0.44). The low negative charge is undoubtedly tied to strong back bonding from the negatively charged Mo atom to the strong π-acceptor AlMe.

The structural relationship between $[Mo(AlMe)_6]$ and $[Rh(AlMe)_4]^+$ is intriguing, since the former is trigonal prismatic and the latter has the structure of a trigonal prism with two vacant vertices occupied by lone pairs. Replacing two AlMe ligands in the molybdenum complex by two lone pairs would take us to an isoelectronic $[Pd(AlMe)_4]$, and this complex optimizes to a tetrahedral structure, consistent with a d^{10} electron configuration at the Pd atom. The rhodium compound has two fewer electrons. The trigonal prismatic structure of the four Rh−Al bonds and the two lone pairs (combined with the fact that our calculations point to an effective d^{10} configuration for the Rh atom), may indicate that the two electrons removed on going from $[Mo(AlMe)_6]$ to $[Rh(AlMe)_4]^+$ are taken from the ligands rather than from the metal. We see here support for the inverse ligand field situation.

4. THE SNYDER CASE RECONSIDERED

4.1. Electronic Structure of $[Cu(CF_3)_4]^{n-}$ Complexes

We return to the $[Cu(CF_3)_4]^{n-}$ system for a comprehensive examination of the geometries and the orbitals. Experimentally, the situation has changed from the days of Snyder's examination of the monoanion,[42] as a result of improved access to the monoanion stemming from the efficient synthesis of Grushin and co-workers[44] and from the clever use of core spectroscopies to establish the composition of the orbitals from the Lancaster group.[48,105]

Only the monoanion, formally Cu(III) if we count all the CF_3 ligands as anionic, is known. However, we calculate as well the di- and trianion, for their geometries and orbital compositions are revealing. Throughout this section we refer to the oxidation state of copper in the traditional way, assuming all ligands monoionic.

Figure 15 shows the computed equilibrium geometries of the mono-, di-, and trianion. The monanion is nearly square-planar, the trianion is tetrahedral, and the dianion in-between. The shape-measure estimate of the extent of tetrahedricity[70,71] is given below the structure.

In Figure 16 we show the evolution of the important valence orbitals along the series.

For Cu(II), with a geometry intermediate between square planar and tetrahedral, the high lying t_2-derived orbitals acquire predominant ligand character, while x^2-y^2 becomes the lowest MO of the d block, with metal ligand bonding character. Thus, there is an inverse ligand field already in the Cu(II) complex but not in the Cu(I) analogue.

DOI: 10.1021/acs.chemrev.6b00251
Chem. Rev. 2016, 116, 8173−8192

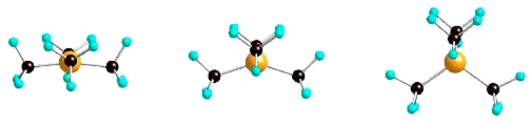

Tetrahedricity (%)	19	54	100
Cu-C (Å)	2.007	2.096	2.188
C-F (Å)	1.366	1.399	1.437

Figure 15. Optimized geometries for the anionic complexes (from left to right) $[Cu(CF_3)_4]^-$, $[Cu(CF_3)_4]^{2-}$, and $[Cu(CF_3)_4]^{3-}$. The tetrahedricity value given under each structure is the generalized coordinate along the square planar to tetrahedron distortion pathway (expressed as a percentage).

To try to ascertain the relative importance of the copper oxidation state and of the coordination geometry on the inversion of the ligand field in the "Cu(II)" and "Cu(III)" cases, we have analyzed the MOs of the three $[Cu(CF_3)_4]^{n-}$ anions at the geometry optimized for the intermediate oxidation state (see SI). In the Cu(I) complex, even if the geometry is intermediate between square planar and tetrahedral, the MO diagram corresponds to an inverse square planar ligand field, in contrast with the normal tetrahedral ligand field the anion has in its optimized geometry (Figure 16, right). This indicates that not only the metal oxidation state but also the geometry has an influence on ligand field inversion. For the Cu(III) complex, however, only minor changes in the MO diagram are observed between the optimized square planar and the constrained intermediate geometry.

Finally, we would like to mention that the predominantly ligand character of the frontier orbitals of these systems had been hinted at, but not explicitly stated, in previous calculations of reductive eliminations from $Au(CH_3)_3$ and $[Au(CH_3)_4]^-$.[106,107]

4.2. Walsh Diagram for Square Planar to Tetrahedral Distortion in $[Cu(CF_3)_4]^{2-}$

Consider a Walsh diagram, relating square planar and tetrahedral geometries through a D_{2d} pathway (Figure 17). Naturally, the composition of the molecular orbitals of the system varies with the total charge on the system. In the interests of simplicity we chose for detailed examination the radical dianion, which actually adopts an intermediate geometry along this deformation trajectory.

The red and blue symbols in Figure 17 label the predominant character (metal vs 4 ligands together) at every point in the Walsh diagram. The actual composition of all of the orbitals in

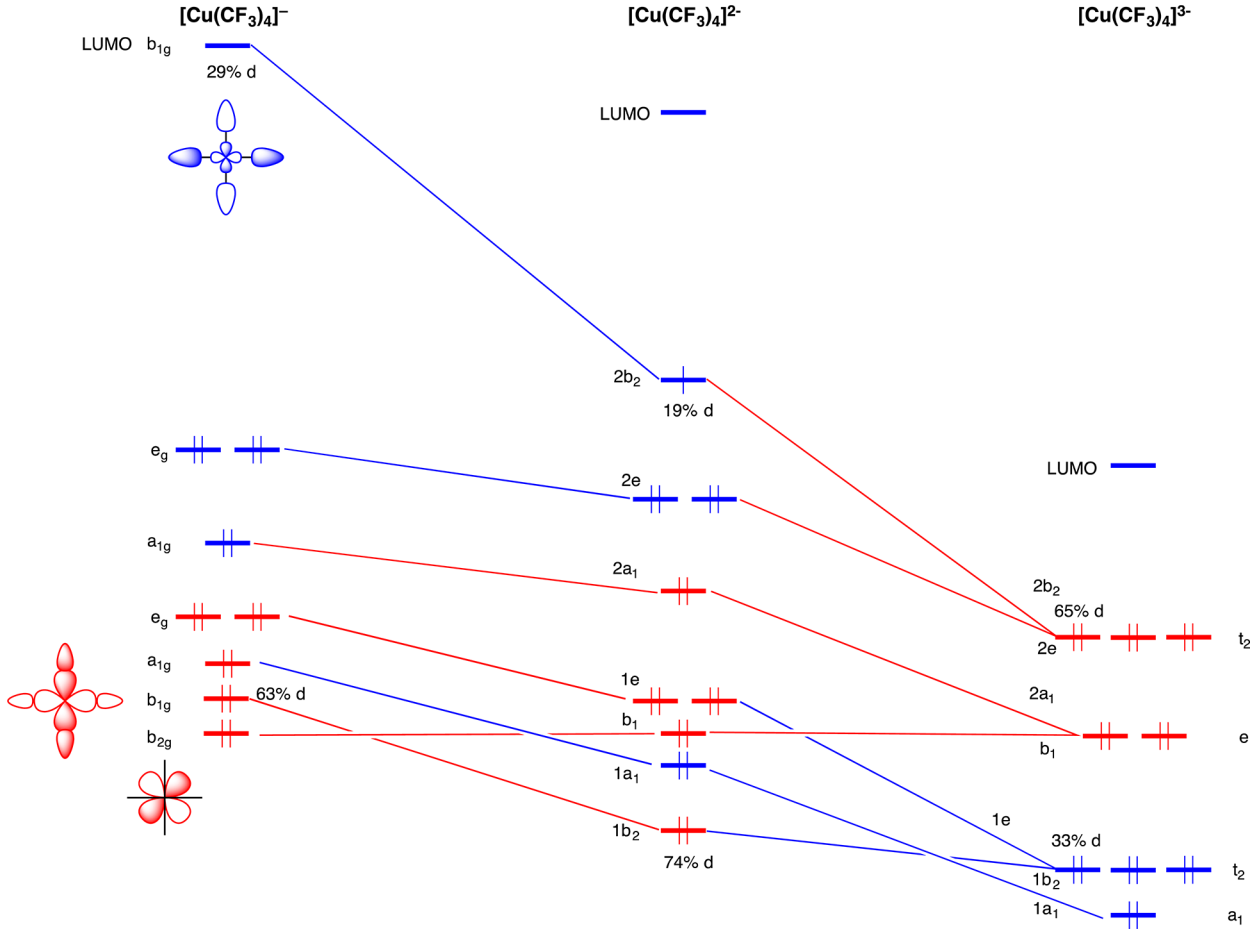

Figure 16. Valence orbitals of $[Cu(CF_3)_4]^{n-}$ in their equilibrium geometries. For the tetrahedral trianion, the orbitals are labeled both in T_d and in the reduced D_{2d} symmetry. The anion is close to square-planar, so D_{4h} labels are used. The absolute energies of the levels would, of course, go up with energy with increasing negative charge on the molecule; in the diagram they are relative to that of the xy orbital for each complex. The specified orbital composition is from a Mulliken population analysis; somewhat different values are obtained from NAO calculations.

DOI: 10.1021/acs.chemrev.6b00251
Chem. Rev. 2016, 116, 8173−8192

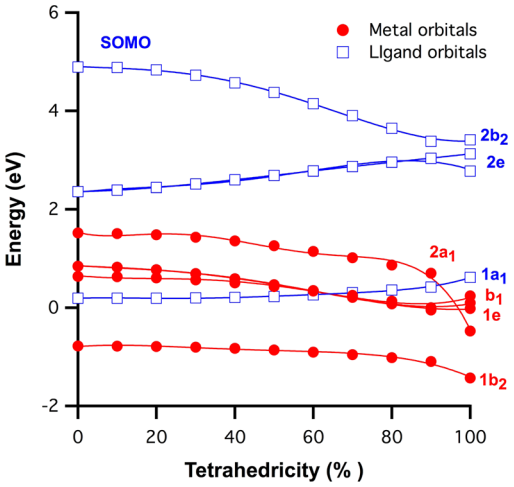

Figure 17. Walsh diagram, computed for $[Cu(CF_3)_4]^{2-}$ along the path from square-planar to tetrahedral. The horizontal coordinate is a measure of tetrahedricity, increasing to the right. The Cu−C and C−F bond distances were optimized at each point along the path. D_{2d} symmetry labels are used, even as the actual symmetry may be lower (as the splittings of the e levels near the tetrahedral extreme show). SOMO = singly occupied molecular orbital.

the diagram is given in the SI; in Figure 18 below we show the relevant information for only one, the b_2 SOMO of the dianion.

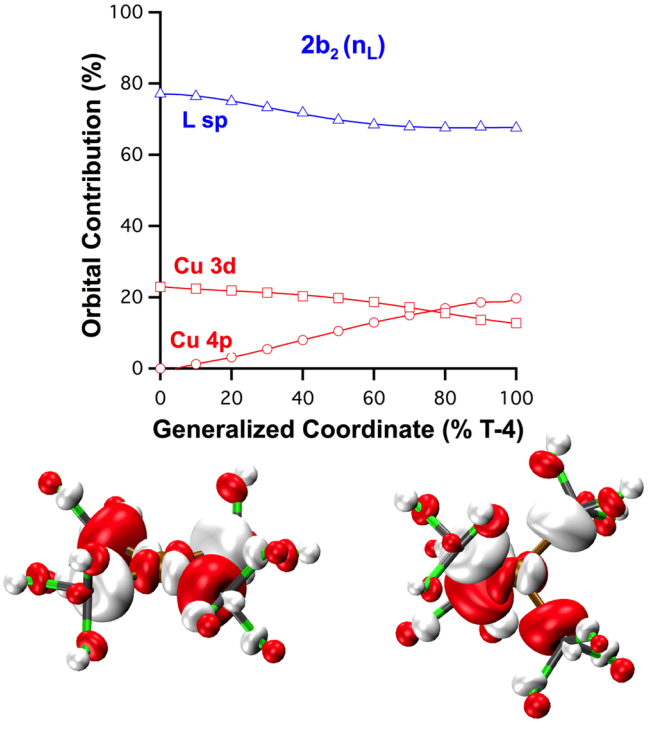

Figure 18. Changes in the atomic orbital contributions to the $2b_2$ SOMO of $[Cu(CF_3)_4]^{2-}$ as it is distorted from square planar to tetrahedral.

The computational observations are clear:

1. The predominantly metal levels are below the predominantly ligand ones; the situation is right for an inversion of the ligand field. This clearly occurs, and governs the composition of the orbitals.

2. The mainly ligand orbitals vary in energy somewhat more than the mainly 3d ones. However, this (higher-lying valence orbitals varying more) is typical of molecules in general.

3. The geometrical preference is set by the higher, mainly ligand orbitals. If the $2b_2$ SOMO of $[Cu(CF_3)_4]^{2-}$ is vacated (Figure 17), it is clear that there will be a trend toward square planarity.

4. The $2b_2$ SOMO of $[Cu(CF_3)_4]^{2-}$ has mostly ligand character, mixed with a significant contribution from x^2-y^2 in the square planar conformation, while a comparable amount of Cu 4p hybridization is incorporated as the anion is distorted toward a tetrahedron (Figure 18).

The question remains: What is being oxidized in $[Cu(CF_3)_4]^-$: the metal or the ligands?

4.3. Consequences, in Charge Distribution, Geometry, and Reactivity

There is no problem with one ligand in $[Cu(CF_3)_4]^-$ being formally CF_3^+, the others CF_3^- (or for that matter two being $CF_3^\bullet$), and yet approximate 4-fold symmetry maintained; considerations of resonance in benzene or ozone have long taught us not to get hung up on this. A question remains, or rather two: Can we see the effects of such an electron assignment, even as we recognize it as a formality, in the charge distribution or the geometry, and what are the thermochemical, structural, and reactivity consequences of having an oxidized ligand?

4.3.1. Electron Distribution. On the first point, with cognizance of the ambiguity of any electron partitioning, we give in Table 3 the division of the electron density (measured by natural population analysis)[108,109] between Cu and the four CF_3 ligands in the equilibrium geometries of two anions. The Cu in the monoanion is positive, and the charge on each CF_3 is down from −1. As one moves to the trianion, approximately one electron goes to the ligands and one to the copper. However, we do not judge the electron distribution analysis to provide definitive evidence for ligand oxidation in $[Cu(CF_3)_4]^-$.

Table 3. Natural Atomic (Group) Charges in $[Cu(CF_3)_4]$ Anion and Trianion

	$[Cu(CF_3)_4]^-$	$[Cu(CF_3)_4]^{3-}$
Cu	0.74	−0.27
CF_3	−0.44	−0.68

In the SI we provide a detailed comparative analysis with $[Cu(CH_3)_4]^{-,\,3-}$.

4.3.2. Ligand Geometry. The computed geometries for CF_3^+ through the radical to CF_3^- are shown in Figure 19 below.[110,111] We have also put in an optimization of an unreal $CF_3^{-0.5}$, which represents the average charge level for $(CF_3^-)_3(CF_3^+)$. The trend is as expected; the more negative the CF_3, the more pyramidal the species and the longer the CF bonds.

As we saw in Figure 15, the optimized C−F distance in SP-$[Cu(CF_3)_4]^-$ is 1.37 Å; in T_d-$[Cu(CF_3)_4]^{3-}$ it is 1.44 Å; the C−F−C angles are 105 and 100° in the two ions, respectively. The correspondence with expectations for $(CF_3^-)_3(CF_3^+)$ and $(CF_3^-)_4$ is striking.

4.3.3. What is Being Oxidized? In Grushin's preparation of $[Cu(CF_3)_4]^-$, O_2 in the air performs a $2e^-$ oxidation at some point after the addition of the CF_3^- anions, released from

DOI: 10.1021/acs.chemrev.6b00251
Chem. Rev. 2016, 116, 8173−8192

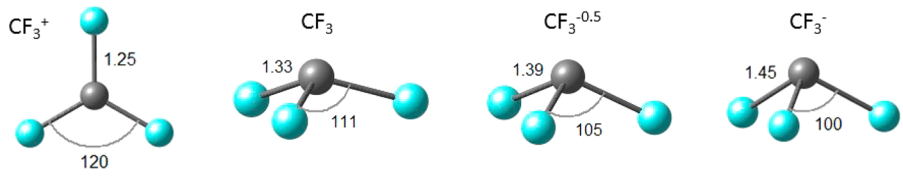

Figure 19. Calculated optimum geometries for CF_3 ligands with a variable charge.

Me_3SiCF_3, to the linear complex $[Cu(CF_3)_2]^-$ or its metastable precursor, $Cu(CF_3)$. We have simulated the thermochemical aspects of this oxidation, but for another oxidant, I_2.[112] The results of the B3LYP calculations with the PCM model of the solvent CH_2Cl_2, used to screen the charges, are summarized in Table 4. We assumed as the redox precursor of SP-$[Cu(CF_3)_4]^-$, the tetrahedral complex T_d-$[Cu(CF_3)_4]^{3-}$.

Table 4. Thermochemical Data for Selected Reactions Related to $[Cu(CF_3)_4]^-$[a]

eq	reaction	$\Delta G/\Delta E$ (kcal mol^{-1})
1	T_d-$[Cu(CF_3)_4]^{3-}$ + I_2 → SP-$[Cu(CF_3)_4]^-$ + $2I^-$	−91/−97
2	T_d-$[Zn(CH_3)_4]^{2-}$ + I_2 → SP-$[Zn(CH_3)_4]$ + $2I^-$	−84/−90
3	CF_3^- + I_2 → CF_3^+ + $2I^-$	+22/+24
4	CF_3^+ + I^- → CF_3I	−67/−74
5	T_d-$(CF_3)_4^{4-}$ → SP-$(CF_3)_4^{4-}$	n.a./+109
6	SP-$(CF_3)_4^{4-}$ + I_2 → SP-$(CF_3)_4^{2-}$ + $2I^-$	n.a./−221
7	SP-$[Cu(CF_3)_4]^-$ → TP-$[Cu(CF_3)_3]^{2-}$ + CF_3^+	+90/+111
8	SP-$[Cu(CF_3)_4]^-$ + PH_3 → $[Cu(CF_3)_3]^{2-}$ + $[H_3PCF_3]^+$	+47/+54
9	SP-$[Cu(CF_3)_4]^-$ + F^- → TP-$[Cu(CF_3)_3]^{2-}$ + CF_4	−29/−18

[a]The energy values, obtained from DFT/B3LYP calculations by using the CPCM CH_2Cl_2 solvent model, are given as both free energies ΔG (when available from full optimization) and electronic energies ΔE. Geometry labels: SP is square planar, T_d is tetrahedral, and TP is trigonal pyramidal.

The large free energy change (ΔG = −91 kcal mol^{-1}) in iodine oxidation (eq 1 of Table 4) is consistent with the known high stability of the product, but does not tell us whether the two removed electrons belong to the metal or the ensemble of the ligands. In this respect, the related pair of zinc complexes T_d-$[Zn(CH_3)_4]^{2-}$ and SP-$[Zn(CH_3)_4]$ is highly informative. The CH_3 ligands were used for two reasons: the T_d X-ray crystal structure of the dianion is known[113] and also the CF_3 equivalent, which would be strictly isoelectronic with the Cu complexes, does not optimize in our calculations in the tetrahedral form. Below we discuss the (significant) difference between CH_3 and CF_3 ligands for both Cu and Zn.

Why study the Zn complex? While one could imagine in the cuprate case oxidation at the metal, one is unlikely to countenance that for $[Zn(CH_3)_4]^{2-}$ going to $[Zn(CH_3)_4]$ − Zn(IV) is unlikely. As Table 4 shows, the different ligands (CH_3 vs CF_3) do not dramatically affect the redox energy trends, since the oxidation of T_d-$[Zn(CH_3)_4]^{2-}$ with I_2 (eq 2) is slightly less exergonic than that of the corresponding Cu one (−84 vs −91 kcal mol^{-1}). Moreover, the geometry of the unknown SP-$[Zn(CH_3)_4]$ species is very similar to the SP-$[Cu(CH_3)_4]^-$ one. Thus, the comparison between the Zn and Cu systems corroborates the feasibility of the ligand centered $2e^-$ oxidation.

Equations 3 and 4 address the energetics of CF_3^- oxidation with I_2. The isolated CF_3^+ unit seems disfavored by the positive ΔG of +22 kcal mol^{-1}, but then oxidation is more than compensated by an assisting base such as I^- to form the product CF_3I (ΔG = −67 kcal mol^{-1}). This reaction is feasible; it is worth mentioning that the I_2 addition to a carboanion of the type R^-Li^+ is a known synthetic strategy to obtain iodo-compounds.[114] The electron transfer involved has been recently illustrated to go through a dynamic halogen bonding adduct.[115]

Another strategy was adopted to explore the nature of the electrons removed by the oxidant in eq 1 with formation of SP-$[Cu(CF_3)_4]^-$. The idea was to take the set of ligands alone, viewed as monoanionic CF_3^- bases, and compare their oxidation to that of the molecules formed with a centering Cu atom. In implementing this approach, we could only calculate the single-point electronic energies (E) of the pure ligand assemblies T_d-$(CF_3)_4^{4-}$, SP-$(CF_3)_4^{4-}$, and SP-$(CF_3)_4^{2-}$ in the geometry they have in the optimized cuprate complexes T_d-$[Cu(CF_3)_4]^{3-}$ and SP-$[Cu(CF_3)_4]^-$. Expectedly, the T_d → SP rearrangement of four CF_3^- anions alone (eq 5 in Table 4) was found to have a large electronic energy cost (ΔE = +109 kcal mol^{-1}). This is consistent with either a pure electrostatic argument, or with an orbital one, the Pauli repulsion between the in-pointing σ lone pairs of the CF_3^- anions.

Square-planar $(CF_3)_4^{4-}$ has a very high-lying, and populated, b_{1g} (D_{4h} symmetry label, real symmetry slightly lower) molecular orbital. We will show it soon. So it is not surprising that the removal with I_2 of $2e^-$ to give SP-$(CF_3)_4^{2-}$ is dramatically favored (ΔE = −221 kcal mol^{-1} for eq 6 in Table 4). Combining eqs 5 and 6, we get a ligand only oxidation, T_d-$(CF_3)_4^{4-}$ + I_2 → SP-$(CF_3)_4^{4-}$ + $2I^-$, whose ΔE of −111 kcal/mol^{-1} roughly compares with that for the oxidation of the complex T_d-$[Cu(CF_3)_4]^{3-}$ (ΔE = −97 kcal/mol^{-1} in eq 1). The somewhat different estimates are due to the uncertainty of unoptimized ligand-only species, but the overall result confirms that the $2e^-$ oxidation of the complex is essentially ligand-centered.

There are some further implications of the ligand-only perspective, now on potential ligand−ligand C−C bonding in SP-$[Cu(CF_3)_4]^-$ (related to Al−Al bonding in the complexes we explored earlier). Consider the partial interaction diagram for formation of the complex, Figure 20. Vacation of the high-lying b_{1g} actually affords some delocalized C_4 bonding. This is supported by the computed positive C−C Wiberg indices (+0.19) for SP-$(CF_3)_4^{2-}$, in spite of the rather large C···C distances of 2.85 Å. Hence, the dashed lines drawn between the adjacent C atoms.[116]

By inserting the central metal atom (left side of Figure 19), three C → Cu dative bonds involve the s, p_x, and p_y acceptor orbitals, as previously illustrated also in Figures 7 and 12. The C−C bond index decreases (relative to the ligand only six-electron system) due to some π-backdonation from x^2-y^2 into the antibonding b_{1g} level, but the value does not vanish (it moves from 0.19 to 0.04). The residual C_4 bonding is very weak in SP-$[Cu(CF_3)_4]^-$ but stronger in the electronically

DOI: 10.1021/acs.chemrev.6b00251
Chem. Rev. 2016, 116, 8173−8192

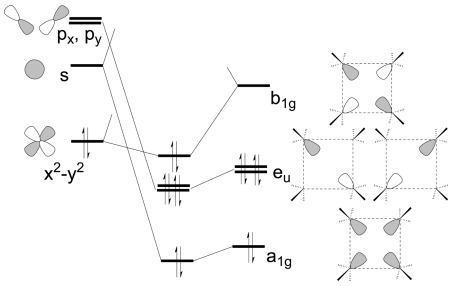

Figure 20. Diagram for the interaction between a naked Cu^+ ion (left side) and the SP-$(CF_3)_4^{2-}$ assembly seen as a C_4 ring. The orbital labels are for D_{4h} symmetry; the symmetry of the complex, of course, is slightly lower.

comparable $[Rh(AlMe)_4]^+$ species, since the Al–Al overlap populations at the Al_4 ring are +0.155. This, probably, is a result of the more diffused Al σ hybrids vs the corresponding C ones.

The picture of primarily ligand-centered oxidation and Cu-back-donation in $[Cu(CF_3)_4]^-$ is consistent with the calculated atomic charges, the trend of structural changes, and the thermochemistry of oxidation in the trianion-to-monoanion conversion.

4.3.4. Electrophilic Reactivity of a CF_3 Ligand. We examine explicitly the thermochemistry of removal of one CF_3, as a Lewis acid, which according to eq 7 of Table 4 is very much uphill energetically (ΔG = +90 kcal mol^{-1}). On the other hand, it is likely that a strong Lewis base favorably assists the CF_3^+ extraction. First, we tried with the simplest phosphine, PH_3, but the reaction between $[Cu(CF_3)_4]^-$ and PH_3 to give the phosphonium cation $[H_3PCF_3]^+$ and the trigonal planar complex $[Cu(CF_3)_3]^{2-}$[117] is quite endergonic (+47 kcal mol^{-1} for eq 8 in Table 4). Shifting of the equilibrium to the right side of the reaction is difficult; we nevertheless investigated the reaction, now assuming an S_N2 mechanism. The latter, which is often associated with organocuprate chemistry, has been addressed also by other theoreticians.[118,119] The transition state calculated is shown in Figure 21a, but the barrier of +79 kcal mol^{-1} argues against the phosphine as an efficient CF_3^+ extractor.

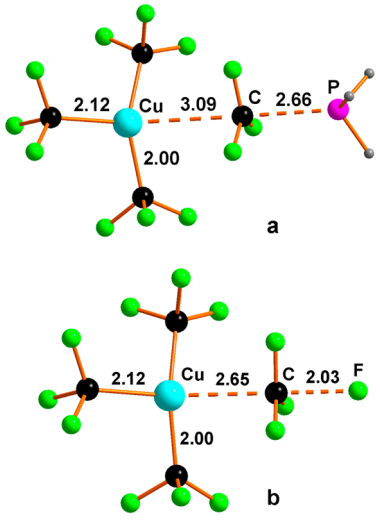

Figure 21. Optimized structure of transition states on the S_N2 pathways: (a) $[Cu(CF_3)_4PH_3]_{TS}^-$ and (b) $[Cu(CF_3)_4F]_{TS}^{2-}$.

Fluoride anions are possible alternatives, as these allow the formation of a new C–F bond, which is the strongest known in organic chemistry. In particular, the formation energy of such bonds is maximized (ΔG = −123 kcal mol^{-1}) in the presence of other F atoms, as is the case of tetrafluoromethane,[120] which is also a product in eq 9 in Table 4. Indeed, the CF_3^+ extraction is now significantly exergonic (ΔG = −29 kcal mol^{-1}), although the optimized S_N2 transition state $[Cu(CF_3)_4F]_{TS}^{2-}$ of Figure 21b still corresponds to a barrier of +56 kcal mol^{-1}. Even if the latter potentially requires drastic thermal conditions to be observed, we are not deterred; computational attempts to lower this reaction barrier, with different substituents, are in progress.

We think there is an acid reaction chemistry waiting to be explored for these unusual complexes, and for other inverted ligand field situations as well.

5. OXIDATION STATE WARS?

The experimental work of Lancaster et al.[48] establishes for $[Cu(CF_3)_4]^-$ quite complete occupation of all five 3d orbitals. With full cognizance of the ambiguity inherent in any definition of oxidation state, two of the authors of this paper (R.H. and C.M.) prefer to think of the monoanion as having copper in oxidation state I. Two other authors (S.A. and A.F.) see the copper as Cu(III). Let us call the remaining authors neutral.

There is nothing wrong with coauthors of a paper disagreeing with each other. While uncommon, with such disagreement typically suppressed in the hierarchical nature of the way that papers get written, in some way this disagreement is a reflection of the creative scrambling for understanding that science at the frontiers represents.

We're friends, so let us see if we can make clearer some of the middle ground between the two views.

The Cu(I) side (to use a football metaphor) of the argument would seem at first glance to be faced with a problem: the characteristic stereochemical signature of a d^{10} system, namely tetrahedricity (as for $[Ni(CO)_4]$ or $[Zn(NH_3)_4]^{2+}$) is absent. The monoanion is near square-planar. While there are a number of square-planar d^{10} complexes, mainly Ag(I),[121] but a few Cu(I),[122,123] the majority of such structures follows the tetrahedral paradigm.[124] The concern that leads that side astray is a phantom; $[Cu(CF_3)_4]^-$ is not an 18-electron molecule but a 16-electron one. In $[Ni(CO)_4]$ or $[Zn(NH_3)_4]^{2+}$ one has ten electrons from the metal and 4 × 2 from the Lewis base ligands. In $[Cu(CF_3)_4]^-$, viewed as Cu(I), one has 10 electrons from the metal, and only 6 from the ligands, precisely as Snyder suggested.[125]

The orbital compositions of Figure 6, though for the dianion, clearly support this view; there are 3 primarily ligand MOs and 5 primarily metal d. The Cu(I) side argues that the orbitals of $[Cu(CF_3)_4]^-$ in their composition resemble less those of a d^8 square-planar transition metal complex than they do a main group EL_4 system with six valence electrons on top of a low-lying filled d-block, say $GaMe_4^+$, formally valence-isoelectronic with $[Cu(CF_3)_4]^-$. The details of the analogy are traced in the SI.

The Cu(III) side argues that a complex with an inverse ligand field is expected to show the same geometrical preferences than those with normal ligand fields, dependent on the effective number of valence electrons and on the σ and π donor characteristics of the ligands.[126] The preferred stereochemistry for a given complex is the one that minimizes the energy of the occupied valence molecular orbitals or, equivalently, the one that maximizes the metal–ligand overlap

DOI: 10.1021/acs.chemrev.6b00251
Chem. Rev. 2016, 116, 8173–8192

in those MOs. Then, the geometry dependence of the overlap should remain similar as we fine-tune the ligand field and move from a larger contribution of a metal d orbital to a larger contribution of the ligand donor orbitals. In other words, the geometry-dependence of the overlap for an MO with 60% d-orbital and 40% ligand contribution is roughly the same as for a 40% metal and 60% ligand contribution.

Since the cases in which one can obtain an inverse ligand field are rather limited, the Cu(III) side contends that assigning a formal oxidation state in the classical way (i.e., counting each ligand as a two electron donor) offers a general framework for comparing and understanding the geometries of the coordination spheres. So the $[Cu(CF_3)_4]^{n-}$ complexes could be considered to correspond to formal oxidation states Cu(III) (n = 1), Cu(II) (n = 2), and Cu(I) (n = 3). Even if in the former case there is spectroscopic and computational evidence for a d^{10} configuration, its bonding and stereochemistry are as expected for a formal oxidation state of +3 (i.e., a d^8 configuration), with a square planar geometry and short Cu−C bond distances (2.01 and 1.96 Å calculated and experimental). Unsurprisingly, the formally Cu(I) and Cu(II) complexes present tetrahedral and intermediate geometries, respectively, as expected for d^{10} and d^9 electron configurations. Also the Cu−C bond distances experience the expected lengthening as the oxidation state decreases (Figure 15). Finally, since the trianion is clearly a Cu(I) complex, if we assign the Cu(I) oxidation state to the monoanion, the assignment of an oxidation state to the dianion becomes problematic.

Both sides agree that in the end, independent of the metal oxidation state, the geometry of the system is governed by the total number of available electrons (16 or 17 or 18), even as the subdivision of the electrons may differ depending on the properties of the metal and the ligands.

Returning to orbital compositions, both sides in the argument agree that inorganic chemists better get used to the idea that even if a simplistic oxidation state line of reasoning would lead you to think a certain orbital should be relatively empty (x^2-y^2 in a 16-electron complex), it may in fact be substantially populated. That holds whether you have a normal or inverted ligand field, but certainly this is true in abundance for the inverted field case.

Jim Snyder deserves full credit for making us aware of this.

Our clever colleagues are certain to come up with foolproof experimental or theoretical measures of oxidation state, which (they will say) will banish our vacillations to the dustbin of history. Why do we have the feeling that chemists will stay with the productive ambiguity we explore?

6. TRANSITION METAL TO MAIN GROUP CHEMISTRY

Molecules do what comes naturally; it is we who, in our struggle to understand them, pigeonhole them into rigid categories and eventually run into trouble. The bonding in transition metal vs main group compounds is an example in point. For instance, if we are asked to decide whether a hypothetical $[Ni(CH_3)_4]^{4-}$ were tetrahedral or square planar, we might build a typical picture of d-block orbitals of Ni(0) interacting with four methyl anion Lewis bases, and draw a mainly d-orbital-based Walsh diagram to reach the conclusion that it should be tetrahedral. If asked to do a bonding analysis for $Ge(CH_3)_4$, we would not worry at all about the core-like 3d orbitals but build a Walsh diagram based on the angular proclivities of the four filled MOs formed pretty much covalently from Ge 4s and 4p, and CH_3 orbitals.[127]

However, $[As(CH_3)_4]^+$, $Ge(CH_3)_4$, $[Ga(CH_3)_4]^-$, $[Zn(CH_3)_4]^{2-}$, $[Cu(CH_3)_4]^{3-}$, and $[Ni(CH_3)_4]^{4-}$, and for that matter the very hypothetical $[Co(CH_3)_4]^{5-}$ and $[Fe(CH_3)_4]^{6-}$, are strictly isoelectronic. Or, if we wanted to stay with all experimental structures, so is the series from AsH_4^+ through CoH_4^{5-}.[128−130] There must be a continuum of bonding in these molecules, influenced in part by the charge on the overall anion (screened, to be sure, by countercations), and the evolution in energy and ability to overlap of the underlying atomic levels. The 3d core clearly sinks in energy as one moves to the right in the periodic table. It is not just the metal that influences the bonding; the donor abilities of ligands make a difference.

A reviewer of our paper has aptly summarized the mind-set at work in our community by writing "In the last 50 years we have slowly discovered that ligands are not as innocent as Werner originally proposed...The idea that transition metals may be as non-innocent has not received the same currency as that given to non-innocent ligands". The reviewer pointed us to some references early on in the development of coordination and organometallic chemistry that worry explicitly about the relative energies and wave functions as one moves across the right side of the transition series and into the main groups.[92]

On innocence: the reviewer points appropriately to the growing realization, good for chemistry, of the noninnocence of some ligand−metal combinations. The classic cases−dithiolenes, bipyridyls, and porphyrins−involve the π MOs of the ligands.[131,132] The cases we have traced around $[Cu(CF_3)_4]^-$ and that led us to this general problem (see section 1.4) can be termed instances of σ-noninnocence. We have a feeling they are more common than one imagines.

The question remains: When in our considerations of bonding in this series do we switch from transition metal thinking, focusing on 3d levels, to main group thinking, focusing on 4s and 4p? It has to be around Cu and Zn, and we have trouble, given our dichotomizing ways, of making this switch. We think that our discussion of $[Cu(CF_3)_4]^-$ in particular, and inverted ligand fields in general, has helped us bring this problem out in the open.

ASSOCIATED CONTENT

Supporting Information

The Supporting Information is available free of charge on the ACS Publications website at DOI: 10.1021/acs.chemrev.6b00251.

Further discussion of $Fe(CO)_4H_2$; further attempts to find an inverted ligand field in tetrahedral complexes; a discussion of which is a better base, CH_3^- or CF_3^-; the analogy between $[Cu(CF_3)_4]^-$ and the $GaMe_4^+$ cation; orbital composition of the $[Cu(CF_3)_4]^{n-}$ anions (n = 1−3); and computational details from the Florence, Barcelona, and Cornell-Ottawa groups. (PDF)

AUTHOR INFORMATION

Corresponding Author

*E-mail: rh34@cornell.edu.

Notes

The authors declare no competing financial interest.

DOI: 10.1021/acs.chemrev.6b00251
Chem. Rev. 2016, 116, 8173−8192

Biographies

Roald Hoffmann received his Ph.D. with Martin Gouterman and William Lipscomb at Harvard in 1962. During his Junior Fellowship at Harvard, 1962−65, he and R. B. Woodward developed the complex of calculations, frontier orbital arguments, and perturbation theory reasoning known as orbital symmetry control in organic reactions. Importantly for what he and his co-workers did in subsequent years (since 1965 he has been at Cornell University), in this period he was transformed from a calculator to an explainer—a process enhanced by teaching introductory chemistry at Cornell. Over the years, Roald has moved from applying his ideas and calculations to organic molecules, then to inorganic and organometallic ones and on to extended structures of every dimensionality. One might also look in his recent work for how an explainer adjusted to the age of quantum chemical simulation.

Santiago Alvarez (born in Panamá, 1950) studied chemistry in the University of Barcelona, where he obtained a Ph.D. under the supervision of Prof. Jaume Casabó. After a postdoctoral stay with Roald Hoffmann at Cornell University in 1983−1984, he became Associate Professor at the University of Barcelona in 1985, and full professor in 1987. He has developed theoretical research on bonding, stereochemistry, and magnetic properties of transition metal compounds. In recent years he has made contributions to the application of continuous shape and symmetry measures to stereochemical studies and to the establishment of structure−properties correlations.

Carlo Mealli got his degree in chemistry at the University of Florence (1969). He continued to master X-ray structure determination techniques in the U.S. with Professors E. C. Lingafelter (UW) and J. A. Ibers (Northwestern). In 1972, he entered the CNR Institute of Organometallic Chemistry in Florence (ICCOM), where he reached top qualification and officially retired from in 2011, but afterwards continued research as an associate. In view of the link between geometry, stereochemistry, electronic properties, and chemical reactivity, he decided to master MO theory by associating with R. Hoffmann since 1980. Soon, he developed the package CACAO for graphic illustrations of perturbation theory principles from EHMO calculations, but generally applicable also to the modern DFT results. His basic interests in chemical bonding and reactivity have produced many contributions spanning organic, organometallic, and main group compounds.

Andrés Falceto (born in Barbastro, 1989) got his B. A. degree in Chemistry at the University of Barcelona. He became a member of the Electronic Structure group in 2011, where he is currently pursuing his Ph.D degree in Chemistry under the supervision of Prof. Santiago Álvarez. He visited Roald's Hoffmann group at Cornell University in 2014. He is working on the symmetry content of the molecular orbitals and its relationship with bonding and electronic structure in different inorganic complexes.

Thomas J. Cahill III was born in Massachusetts where he attended Middlesex School, and received his B.S. in Chemistry (2009) from Hobart College. As an undergraduate, he performed research at Cornell University with Roald Hoffmann. He then received his M.S. in Chemistry (2011) from Stanford University working in the lab of Richard Zare. He is currently in the process of completing an M.D./Ph.D. (MSTP) at Duke University. His Ph.D. work, under the guidance of Robert Lefkowitz, focuses on the biophysical and structural properties of G protein-coupled receptors and their transducers.

Tao Zeng received his B.Sc. in applied chemistry from Jinan University in 2002 and M.Sc. in physical chemistry in 2005 from the Institute of Coal Chemistry, Chinese Academy of Sciences, under the supervision of Professor Haijun Jiao. He received his Ph.D. in computational chemistry in 2011 from the University of Alberta, where he joined Professor Mariusz Klobukowski's group and concentrated on spin−orbit coupling and pseudopotential methods. He then worked with Professor Pierre-Nicholas Roy at the University of Waterloo (2011−2013) and Professors Nandini Ananth and Roald Hoffmann at Cornell University (2013−2015) as a postdoctoral researcher, performing theoretical studies on microscopic superfluid clusters and excited state chemistry, respectively. He became an assistant professor in the Department of Chemistry, Carleton University in July 2015. Research in his group (http://carleton.ca/ccg) involves theoretical studies on optoelectronics and relativistic effects in chemistry.

Gabriele Manca obtained his Ph.D. degree in Chemical Sciences from the University of Pisa in 2009. After a postdoctoral stay at the University of Rennes I with Prof. J.-F. Halet, he joined the group of Dr. C. Mealli at the CNR-ICCOM in Florence, where he mastered applied computational chemistry. He investigated the relations between electronic structure and reactivity of several organometallic species but also examined catalytic processes involving radical activity. Currently, he has a fixed term position to perform research on phosphorene chemistry within the European Research Council grant assigned to Dr. M. Peruzzini (director of ICCOM). The focus is on new 2D materials, exploring possible functionalization (including with transition metal fragments), in the process exploiting the predictive power of computational chemistry.

ACKNOWLEDGMENTS

We have benefitted from discussions with Kyle Lancaster. R.H. is grateful to the National Science Foundation for the support of this work through Research Grant CHE-1305872 and to Yuta Tsuji for some calculations. T.Z. thanks Carleton University for his start-up fund. Research at Barcelona is supported by MINECO through grant CTQ2015-64579-C3-1-P. The Florence group acknowledges the ISCRA-CINECA HP grant "HP10BNL89W" and Centro Ricerca Energia e Ambiente, Colle Val d'Elsa for computational resources.

REFERENCES

(1) Bethe, H. Termaufspaltung in Kristallen. *Ann. Phys.* **1929**, *395*, 133−208.
(2) Gorter, C. J. Note on the Electric Field in Paramagnetic Crystal. *Phys. Rev.* **1932**, *42*, 437−438.
(3) Figgis, N. B. *Introduction to Ligand Fields*; Wiley-Interscience: New York, 1991.
(4) Ballhausen, C. J. *Introduction to Ligand Field Theory*; McGraw-Hill: New York, 1962.
(5) Schläfer, H. L.; Gliemann, G. *Basic Principles of Ligand Field Theory*; Wiley-Interscience: New York, 1969.
(6) Burdett, J. K. New Method for the Determination of the Geometries of Binary Transition Metal Complexes. *Inorg. Chem.* **1975**, *14*, 375−382.
(7) Jørgensen, C. K. Recent Progress in Ligand field Theory. *Struct. Bonding (Berlin)* **1966**, *1*, 3−31.
(8) Schäffer, C. F.; Jørgensen, C. K. The Angular Overlap model, an Attempt to Revive the Ligand Field Approaches. *Mol. Phys.* **1965**, *9*, 401−412.
(9) Albright, T. A.; Burdett, J.; Whangbo, M.-H. *Orbital Interactions in Chemistry*, 2nd ed.; Wiley: Hoboken, NJ, 2013; p 403.
(10) Weinhold, F.; Landis, C. R. *Valency and Bonding: A Natural Bond Orbital Donor-Acceptor Perspective*; Cambridge Univ. Press: Cambridge, U.K., 2005; pp 365−387.
(11) Maseras, F.; Morokuma, K. Application of the Natural Population Analysis to Transition-metal Complexes. Should the

DOI: 10.1021/acs.chemrev.6b00251
Chem. Rev. 2016, 116, 8173−8192

Empty Metal p Orbitals Be Included in the Valence Space? *Chem. Phys. Lett.* **1992**, *195*, 500−504.
(12) Bayse, C. A.; Hall, M. B. Prediction of the Geometries of Simple Transition Metal Polyhydride Complexes by Symmetry Analysis. *J. Am. Chem. Soc.* **1999**, *121*, 1348−1358.
(13) Diefenbach, A.; Bickelhaupt, F. M.; Frenking, G. The Nature of the Transition Metal-Carbonyl Bond and the Question about the Valence Orbitals of Transition Metals. A Bond-Energy Decomposition Analysis of $TM(CO)_6^q$ (TM^q = Hf^{2-}, Ta^-, W, Re^+, Os^{2+}, Ir^{3+}). *J. Am. Chem. Soc.* **2000**, *122*, 6449−6458.
(14) van Vleck, J. H. Valence Strength and the Magnetism of Complex Salts. *J. Chem. Phys.* **1935**, *3*, 807−813.
(15) Orgel, L. E. *An Introduction to Transition-Metal Chemistry: Ligand-Field Theory*; Methuen: London, 1960.
(16) Moffitt, W.; Ballhausen, C. J. Quantum Theory. *Annu. Rev. Phys. Chem.* **1956**, *7*, 107−136.
(17) Cirera, J.; Alvarez, S. How High the Spin? Allowed and Forbidden Spin States in Transition-Metal Chemistry. *Angew. Chem., Int. Ed.* **2006**, *45*, 3012−3020.
(18) Zheng, C.; Hoffmann, R. Conjugation in the 3-Connected Net: the Aluminum Diboride and Thorium Disilicide Structures and their Transition-Metal Derivatives. *Inorg. Chem.* **1989**, *28*, 1074−1080.
(19) Oana, M.; Hoffmann, R.; Abruña, H. D.; Di Salvo, F. J. Adsorption of CO on $PtBi_2$ and PtBi surfaces. *Surf. Sci.* **2005**, *574*, 1−16.
(20) Grochala, W.; Hoffmann, R. Real and Hypothetical Intermediate-Valence Ag^{II}/Ag^{III} and Ag^{II}/Ag^{I} Fluoride Systems as Potential Superconductors. *Angew. Chem., Int. Ed.* **2001**, *40*, 2742−2781.
(21) Leszczyński, P. J.; Grochala, W. Strong Cationic Oxidizers: Thermal Decomposition, Electronic Structure and Magnetism of Their Compounds. *Act. Chim. Slov.* **2013**, *60*, 455−470.
(22) Grochala, W.; Mazej, Z. Chemistry of Silver(II): a Cornucopia of Peculiarities. *Philos. Trans. R. Soc., A* **2015**, *373*, 20140179.
(23) Grochala, W.; Egdell, R. G.; Edwards, P. P.; Mazej, Z.; Žemva, B. On the Covalency of Silver−Fluorine Bonds in Compounds of Silver(I), Silver(II) and Silver(III). *ChemPhysChem* **2003**, *4*, 997−1001.
(24) Mealli, C.; Proserpio, D. M. MO Theory Made Visible. *J. Chem. Educ.* **1990**, *67*, 399−402.
(25) Hoffmann, R. Interaction of Orbitals Through Space and Through Bonds. *Acc. Chem. Res.* **1971**, *4*, 1−9.
(26) Mealli, C.; Ghilardi, C. A.; Orlandini, A. Structural Flexibility and Bonding Capabilities of the Ligand np_3 Toward the Transition Metals. *Coord. Chem. Rev.* **1992**, *120*, 361−387.
(27) Midollini, S.; Orlandini, A.; Sacconi, L. Synthesis, Properties and X-ray Structural Determination of Cationic Five-coordinate σ-triphenylstannylnickel (II) Complexes with Poly(tertiary phosphines). *J. Organomet. Chem.* **1978**, *162*, 109−120.
(28) Parkin, G. A Simple Description of the Bonding in Transition-Metal Borane Complexes. *Organometallics* **2006**, *25*, 4744−4747.
(29) Mealli, C.; Sabat, M.; Marzilli, L. G. Coenzyme B12 Cobalt-Carbon Bond Homolysis: Insights from Qualitative Molecular Orbital Theory. *J. Am. Chem. Soc.* **1987**, *109*, 1593−1594.
(30) Bresciani-Pahor, N.; Forcolin, M.; Marzilli, L. G.; Randaccio, L.; Summers, M. F.; Toscano, P. J. Organocobalt B_{12} Models: Axial Ligand Effects on the Structural and Coordination Chemistry of Cobaloximes. *Coord. Chem. Rev.* **1985**, *63*, 1−125.
(31) Lippard, S. J.; Berg, J. M. *Principles of Bioinorganic Chemistry*; Univ. Science Books: Mill Valley, CA,1994; pp 336−343.
(32) Suzuki, H.; Omori, H.; Lee, D. H.; Yoshida, Y.; Moro-oka, Y. A Novel Dinuclear Tetrahydride Bridged Ruthenium Complex, (η^5-C_5Me_5) Ru (μ-H)$_4$ Ru(η^5-C_5Me_5). *Organometallics* **1988**, *7*, 2243−2245.
(33) Koga, N.; Morokuma, K. Ab Initio Study on the Structure and H_2 Dissociation Reaction of a Tetrahydride-bridged Dinuclear Ru Complex, $(C_5H_5)Ru(\mu\text{-}H)_4Ru(C_5H_5)$. *J. Mol. Struct.* **1993**, *300*, 181−189.
(34) Recently Suzuki reported further details of the synthesis of these H-bridged compounds Shimogawa, R.; Takao, T.; Suzuki, H. Synthesis, Characterization, and Reactions of Ruthenium(II), -(III), and -(IV) Complexes with Sterically Demanding 1,2,4-Tri-*tert*-butylcyclopentadienyl Ligands. *Organometallics* **2014**, *33*, 289−301 which starts from Ru(III) (or in one case even Ru(IV)) chloride complexes upon the treatment with borohydrides. Evidently, the process is not limited to simple substitutions of the chloride for the hydride ligands but has redox character in the metal reduction. The latter is not simply based on an inner electron redistribution in going from σ donation to backdonation but seems to involve the reductive power of the borohydrides, which forces the occupation of the highest filled dδ* MO, which is excluded from any interaction with the H bridges (Figure 5).
(35) Llunell, M.; Alvarez, S.; Alemany, P.; Hoffmann, R. Electronic Structure, Bonding, and Electrical Properties of $MoNiP_8$. *Inorg. Chem.* **1996**, *35*, 4683−4689.
(36) Llunell, M.; Alemany, P.; Alvarez, S.; Zhukov, V.; Vernes, A. Electronic Structure and Bonding in Skutterudite-type Phosphides. *Phys. Rev. B: Condens. Matter Mater. Phys.* **1996**, *53*, 10605−10609.
(37) Llunell, M.; Alvarez, S.; Alemany, P. Skutterudite *vs.* ReO_3 structures for MX_3 Solids: Electronic Requirements. *J. Chem. Soc., Dalton Trans.* **1998**, 1195−1200.
(38) Alvarez, S.; Hoffmann, R.; Mealli, C. A Bonding Quandary—or—A Demonstration of the Fact That Scientists Are Not Born With Logic. *Chem. - Eur. J.* **2009**, *15*, 8358−8373.
(39) Jenkins, D. M.; Di Bilio, A. J.; Allen, M. J.; Betley, T. A.; Peters, J. C. Elucidation of a Low Spin Cobalt(II) System in a Distorted Tetrahedral Geometry. *J. Am. Chem. Soc.* **2002**, *124*, 15336−15350.
(40) Jenkins, D. M.; Peters, J. C. Spin-State Tuning at Pseudotetrahedral d^7 Ions: Examining the Structural and Magnetic Phenomena of Four-Coordinate $[BP_3]Co^{II}$−X Systems. *J. Am. Chem. Soc.* **2005**, *127*, 7148−7165.
(41) Brown, S. D.; Peters, J. C. Ground-State Singlet L_3Fe-(μ-N)-FeL_3 and $L_3Fe(NR)$ Complexes Featuring Pseudotetrahedral Fe(II) Centers. *J. Am. Chem. Soc.* **2005**, *127*, 1913−1923.
(42) Snyder, J. P. Elusiveness of Cu^{III} Complexation; Preference for Trifluoromethyl Oxidation in the Formation of $[Cu^{I}(CF_3)_4]^-$ Salts. *Angew. Chem., Int. Ed. Engl.* **1995**, *34*, 80−81.
(43) Naumann, D.; Roy, T.; Tebbe, K.-F.; Crump, W. Synthesis and Structure of Surprisingly State Tetrakis(trifluoromethyl)cuprate(III) Salts. *Angew. Chem., Int. Ed. Engl.* **1993**, *32*, 1482−1483.
(44) Romine, A. M.; Nebra, N.; Konovalov, A. I.; Martin, E.; Benet-Buchholz, J.; Grushin, V. V. Easy Access to the Copper(III) Anion $[Cu(CF_3)_4]^-$. *Angew. Chem., Int. Ed.* **2015**, *54*, 2745−2749.
(45) Kaupp, M.; von Schnering, H. G. Formal Oxidation State versus Partial Charge — A Comment. *Angew. Chem., Int. Ed. Engl.* **1995**, *34*, 986.
(46) Snyder, J. P. Distinguishing Copper d^8 and d^{10} Configurations in a Highly Ionic Complex; A Nonformal Metal Oxidation State. *Angew. Chem., Int. Ed. Engl.* **1995**, *34*, 986−987.
(47) Aullón, G.; Alvarez, S. Oxidation States, Atomic Charges and Orbital Populations in Transition Metal Complexes. *Theor. Chem. Acc.* **2009**, *123*, 67−73.
(48) Walroth, R. C.; Lukens, J. T.; MacMillan, S. N.; Finkelstein, K. D.; Lancaster, K. M. Spectroscopic Evidence for a $3d^{10}$ Ground State Electronic Configuration and Ligand Field Inversion in $[Cu(CF_3)_4]^{1-}$. *J. Am. Chem. Soc.* **2016**, *138*, 1922−1931.
(49) Sarangi, R.; York, J. T.; Helton, M. E.; Fujisawa, K.; Karlin, K. D.; Tolman, W. B.; Hodgson, K. O.; Hedman, B.; Solomon, E. I. X-Ray Absorption Spectroscopic and Theoretical Studies on $(L)_2[Cu_2(S_2)_n]^{2+}$ Complexes: Disulfide versus Disulfide (•1-) Bonding. *J. Am. Chem. Soc.* **2008**, *130*, 676−686.
(50) York, J. T.; Brown, E. C.; Tolman, W. B. Characterization of a Complex Containing a $\{Cu_2(S_2)_2\}^{2+}$ Core: Bis(μ-S_2^{2-})dicopper(III) or Bis (μ-$S_2^{\cdot-}$)dicopper(II)? *Angew. Chem., Int. Ed.* **2005**, No. 44, 7745−7748.

DOI: 10.1021/acs.chemrev.6b00251
Chem. Rev. 2016, 116, 8173−8192

(51) Yvon, K. Hydrides: Solid State Transition Metal Complexes. In *Encyclopedia of Inorganic Chemistry*; King, R. B., Ed.; John Wiley: New York, 1994; Vol. 3, pp 1401−1420.
(52) Bortz, M.; Yvon, K.; Fischer, P. Synthesis and Structure Determination of Complex Zinc Hydrides Part 1: Dipotassiumtetrahydridozincate(II): $K_2[ZnH_4]$. *J. Alloys Compd.* **1994**, *216*, 39−42.
(53) Bortz, M.; Yvon, K.; Fischer, P. Synthesis and Structure Determination of Complex Zinc Hydrides Part 2: Tripotassiumtetrahydridozincate(II) hydride, $K_3[ZnH_4]H$. *J. Alloys Compd.* **1994**, *216*, 43−45.
(54) Huang, B.; Yvon, K.; Fischer, P. $LiMg_2RuH_7$, A New Quaternary Metal Hydride Containing Octahedral $[Ru(H)H_6]^{4-}$ complex anions. *J. Alloys Compd.* **1994**, *210*, 243−246.
(55) Huang, B.; Yvon, K.; Fischer, P. New Iron(II) Complex Metal Hydrides with $SrMg_2FeH_8$ Type Structure. *J. Alloys Compd.* **1995**, *227*, 121−124.
(56) Huang, B.; Yvon, K.; Fischer, P. $LiMg_4Os_2H_{13}$ Containing Double Layers of Octahedral $[Os(II)H_6]^{4-}$ Complexes. *J. Alloys Compd.* **1996**, *245*, L24−L27.
(57) Yvon, K. Complex Transition-Metal Hydrides. *CHIMIA* **1998**, *52*, 613−619.
(58) Rönnebro, E.; Kyoi, D.; Blomqvist, H.; Noréus, D.; Sakai, T. Structural Characterization of $Mg_3CrH_{\sim 6}$ — A New High-Pressure Phase Synthesized in a Multi-Anvil Cell at 8 GPa. *J. Alloys Compd.* **2004**, *368*, 279−282.
(59) Auffermann, G., Bronger, W. Complex Ternary Transition-Metal Hydrides and Hydridometalates. In *Comprehensive Inorganic Chemistry II*; Reedijk, J., Poeppelmeier, K., Eds.; Elsevier: Amsterdam, 2013; Vol. 3, Chapter 21, pp 583−599.
(60) Takagi, S.; Miwa, K.; Ikeshoji, T.; Sato, R.; Matsuo, M.; Li, G.; Aoki, K.; Orimo, S.-i. Hexavalent Hydrogen Complex in Hypothetical Y_2CrH_6. *J. Alloys Compd.* **2013**, *580*, S274−S277.
(61) Hoffmann, R. An Extended Hückel Theory. I. Hydrocarbons. *J. Chem. Phys.* **1963**, *39*, 1397−1412.
(62) To compensate the artificially large electropositivity of the H atom (−8.6 eV), the s orbital was contracted in that case by using a smaller exponent of its 1s orbitals (1.05 vs 1.3).
(63) Glaser, T.; Hedman, B.; Hodgson, K. O.; Solomon, E. I. Ligand K-Edge X-ray Absorption Spectroscopy: A Direct Probe of Ligand-Metal Covalency. *Acc. Chem. Res.* **2000**, *33*, 859−868.
(64) Suljoti, E.; Garcia-Diez, R.; Bokarev, S. I.; Lange, K. M.; Schoch, R.; Dierker, B.; Dantz, M.; Yamamoto, K.; Engel, N.; Atak, K.; et al. Direct Observation of Molecular Orbital Mixing in a Solvated Organometallic Complex. *Angew. Chem., Int. Ed.* **2013**, *52*, 9841−9844.
(65) Hoffmann, R. Hi O Silver. *Am. Sci.* **2001**, *89*, 311−314.
(66) Jørgensen, C. K. *Oxidation Numbers and Oxidation States*; Springer: Berlin, 1969.
(67) Raebiger, H.; Lany, S.; Zunger, A. Charge Self-Regulation Upon Changing the Oxidation State of Transition Metals in Insulators. *Nature* **2008**, *453*, 763−766.
(68) Jansen, M.; Wedig, U. A Piece of the Picture-Misunderstanding of Chemical Concepts. *Angew. Chem., Int. Ed.* **2008**, *47*, 10026−10029.
(69) McNeill, E. A.; Scholer, F. R. Molecular Structure of the Gaseous Metal Carbonyl Hydrides of Manganese, Iron, and Cobalt. *J. Am. Chem. Soc.* **1977**, *99*, 6243−6249.
(70) Drouin, B. J.; Kukolich, S. G. Molecular Structure of Tetracarbonyldihydroiron: Microwave Measurements and Density Functional Theory Calculations. *J. Am. Chem. Soc.* **1998**, *120*, 6774−6780.
(71) In the SI the structural details of the structure determination are shown, along with the results of a DFT calculation. The only significant difference is in the H−Fe−H angle, which is 100° in the electron diffraction structure, and 84° in the calculation.
(72) Alvarez, S.; Alemany, P.; Casanova, D.; Cirera, J.; Llunell, M.; Avnir, D. Shape Maps and Polyhedral Interconversion Paths in Transition Metal Chemistry. *Coord. Chem. Rev.* **2005**, *249*, 1693−1708.
(73) Cirera, J.; Ruiz, E.; Alvarez, S. Continuous Shape Measures as a Stereochemical Tool in Organometallic Chemistry. *Organometallics* **2005**, *24*, 1556−1562.
(74) Dewar, M. J. S.; Ford, G. P. *J. Am. Chem. Soc.* **1979**, *101*, 783−791 and references therein.
(75) Crabtree, R. H. *The Organometallic Chemistry of the Transition Metals*; Wiley: New York, 1988; pp 89−95.
(76) Albright, T. A.; Hoffmann, R.; Thibeault, J. C.; Thorn, D. L. *J. Am. Chem. Soc.* **1979**, *101*, 3801−3812 and references therein.
(77) Mingos, D. M. P. A Review of Complexes of Ambivalent and Ambiphilic Lewis Acid/Bases with Symmetry Signatures and an Alternative Notation for These Non-Innocent Ligands. *J. Organomet. Chem.* **2014**, *751*, 153−173.
(78) Mingos, D. M. P. Ambivalent Lewis Acid/Bases with Symmetry Signatures and Isolobal Analogies. *Struct. Bonding (Berlin, Ger.)* **2014**, *154*, 1−52.
(79) Goesten, M. G.; Guerra, C. F.; Kapteijn, F.; Gascon, J.; Bickelhaupt, F. M. Six-Coordinate Group 13 Complexes: The Role of d Orbitals and Electron-Rich Multi-Center Bonding. *Angew. Chem., Int. Ed.* **2015**, *54*, 12034−12038.
(80) From "To a Mouse," by Robert Burns "The best-laid schemes o′ mice an′ men/Gang aft agley." Burns, R. *Complete poems*; T. Y. Crowell & Co.: New York, 1900; p 37.
(81) Greenwood, N. N.; Earnshaw, A. *Chemistry of the elements*; Butterworth-Heinemann: Oxford, U.K., 1997; Chapter 27.
(82) Cotton, F. A.; Wilkinson, G.; Murillo, C. A.; Bochmann, M. *Advanced Inorganic Chemistry*, 6th ed.; Wiley-Interscience: New York, 1999; Sections 17-G-7 and 18-H-2.
(83) For an early summary, see: Otsuka, S. Chemistry of Platinum and Palladium Compounds of Bulky Phosphines. *J. Organomet. Chem.* **1980**, *200*, 191−205.
(84) For a thorough analysis of this alternative in d^{10} complexes of group 11, see: Carvajal, M. A.; Novoa, J. J.; Alvarez, S. Choice of Coordination Number in d^{10} Complexes of Group 11 Metals. *J. Am. Chem. Soc.* **2004**, *126*, 1465−1477.
(85) The significant difference in the nature between BiH_3 and PH_3 exemplifies a common trend as one moves down in the periodic table, a trend that can be rationalized in different ways. Rahm and Christe have, for instance, shown that electrons within the domain formally associated with the lone pair on BiH_3 are significantly less localized compared to those in the corresponding domain in PH_3: Rahm, M.; Christe, K. O. Quantifying the Nature of Lone Pair Domains. *ChemPhysChem* 2013, *14*, 3714−3725. They have also shown that the electrostatic potential (calculated on an isosurface above the site of the lone pair) is markedly different between the two molecules.10.1002/cphc.201300723
(86) Zhao, Y.; Truhlar, D. G. The M06 Suite of Density Functionals for Main Group Thermochemistry, Thermochemical Kinetics, Noncovalent Interactions, Excited States, and Transition Elements: Two New Functionals and Systematic Testing of Four M06-Class Functionals and 12 Other Functionals. *Theor. Chem. Acc.* **2008**, *120*, 215−241.
(87) Kendall, R. A.; Dunning, T. H.; Harrison, R. J. Electron Affinities of the First-Row Atoms Revisited. Systematic Basis Sets and Wave Functions. *J. Chem. Phys.* **1992**, *96*, 6796−6806.
(88) Woon, D. E.; Dunning, T. H. Gaussian Basis Sets for Use in Correlated Molecular Calculations. III. The Atoms Aluminum through Argon. *J. Chem. Phys.* **1993**, *98*, 1358−1371.
(89) Balabanov, N. B.; Peterson, K. A. Systematically Convergent Basis Sets for Transition Metals. I. All-Electron Correlation Consistent Basis Sets for the 3d Elements Sc-Zn. *J. Chem. Phys.* **2005**, *123*, 064107.
(90) Zeng, T.; Lancaster, K. M.; Ananth, N.; Hoffmann, R. Anomalous Orbital Admixture in Ammine Complexes. *J. Organomet. Chem.* **2015**, *792*, 6−12.
(91) Von Schnering, H. G.; Vu, D.; Peters, K. Refinement of the Scheelite-Type Structures of $CaZnF_4$ and $SrZnF_4$. *Z. Kristallogr. Cryst. Mater.* **1983**, *165*, 305−308.

DOI: 10.1021/acs.chemrev.6b00251
Chem. Rev. 2016, 116, 8173−8192

(92) Green, M. L. H. In *Organometallic Compounds*, 3rd ed.; Coates, G. E., Green, M. L. H., Wade, K., Eds.; Methuen: London, 1968; Vol. 2, pp 1−6.
(93) Mingos, D. M. P. *Essential Trends in Inorganic Chemistry*; Oxford: Oxford, U.K., 1998; pp 275−277.
(94) Uhl, W.; Pohlmann, M.; Wartchow, R. Ni[In{C(SiMe$_3$)$_3$}$_4$]: An Organometallic Nickel-Indium Compound Analogues to [Ni(CO)$_4$]. *Angew. Chem., Int. Ed.* **1998**, *37*, 961−963.
(95) Uhl, W.; Benter, M.; Melle, S.; Saak, W.; Frenking, G.; Uddin, J. Synthesis and Structure of [Ni{Ga-C(SiMe$_3$)$_3$}$_4$] and Quantum-Chemical Verification of Strong π Back-Bonding in the Model Compounds [Ni(EMe)$_4$] (E = B, Al, Ga, In, Tl). *Organometallics* **1999**, *18*, 3778−3780.
(96) Weiss, D.; Winter, M.; Merz, K.; Knüfer, A.; Fischer, R. A.; Fröhlich, N.; Frenking, G. Synthesis, Structure and Bonding Situation of [(dcpe)Pt(InCp*)$_2$] and {(dcpe)Pt[GaC(SiMe$_3$)$_3$]$_2$} — Two Novel Examples of Platinum Complexes of Low Valent Group 13 Metal Species. *Polyhedron* **2002**, *21*, 535−542.
(97) Uhl, W.; Melle, S. Pt[In−C(SiMe$_3$)$_3$]$^{4-}$ a Pt(CO)$_4$ Analogous Compound with a Platinum Atom Tetrahedrally coordinated by Four InR Ligands. *Z. Anorg. Allg. Chem.* **2000**, *626*, 2043−2045.
(98) Cadenbach, T.; Bollermann, T.; Gemel, C.; Fernández, I.; von Hopffgarten, M.; Frenking, G.; Fischer, R. A. Twelve One-Electron Ligands Coordinating One Metal Center: Structure and Bonding of [Mo(ZnCH$_3$)$_9$(ZnCp*)$_3$]. *Angew. Chem., Int. Ed.* **2008**, *47*, 9150−9154.
(99) Cadenbach, T.; Bollermann, T.; Gemel, C.; Tombul, M.; Fernández, I.; von Hopffgarten, M.; Frenking, G.; Fischer, R. A. Molecular Alloys, Linking Organometallics with Intermetallic Hume−Rothery Phases: The Highly Coordinated Transition Metal Compounds [M(ZnR)$_n$] ($n \geq 8$) Containing Organo−Zinc Ligands. *J. Am. Chem. Soc.* **2009**, *131*, 16063−16067.
(100) Cokoja, M.; Gemel, C.; Steinke, T.; Schröder, F.; Fischer, R. A. Insertion Reactions of GaCp*, InCp* and In[C(SiMe$_3$)$_3$] into the Ru−Cl Bonds of [(*p*-cymene)Ru^{II}Cl$_2$]$_2$ and [Cp*Ru^{II}Cl]$_4$. *Dalton Trans.* **2005**, 44−54.
(101) Cadenbach, T.; Gemel, C.; Zacher, D.; Fischer, R. A. Methylgallium as a Terminal Ligand in [(Cp*Ga)$_4$Rh(GaCH$_3$)]$^+$. *Angew. Chem., Int. Ed.* **2008**, *47*, 3438−3441.
(102) Buchin, B.; Gemel, C.; Kempter, A.; Cadenbach, T.; Fischer, R. A. Reaction of Iron and Ruthenium Halogenide Complexes with GaCp* and AlCp*: Insertion, Cp* Transfer Reactions and Orthometallation. *Inorg. Chim. Acta* **2006**, *359*, 4833−4839.
(103) Steinke, T.; Gemel, C.; Cokoja, M.; Winter, M.; Fischer, R. A. Novel RhCp*/GaCp* and RhCp*/InCp* Cluster Complexes. *Dalton Trans.* **2005**, 55−62.
(104) Cremades, E.; Echeverría, J.; Alvarez, S. The Trigonal Prism in Coordination Chemistry. *Chem. - Eur. J.* **2010**, *16*, 10380−10396.
(105) Other square-planar *per*-CF$_3$ transition metal compounds are known, for instance Pt(CF$_3$)$_4$: Menjón, B.; Martínez-Salvador, S.; Gómez-Saso, M. A.; Forniés, J.; Falvello, L. R.; Martín, A.; Tsipis, A. Oxidative Addition of Halogens to Homoleptic Perfluoromethyl or Perfluorophenyl Derivatives of Platinum(II): A Comparative Study. *Chem. - Eur. J.* 2009, *15*, 6371−6382. We have not yet examined the bonding in these.10.1002/chem.200900323
(106) Komiya, S.; Albright, T. A.; Hoffmann, R.; Kochi, J. K. Reductive Elimination and Isomerization of Organogold Complexes. Theoretical Studies of Trialkylgold Species as Reactive Intermediates. *J. Am. Chem. Soc.* **1976**, *98*, 7255−7265.
(107) Komiya, S.; Albright, T. A.; Hoffmann, R.; Kochi, J. K. The Stability of Organogold Compounds. Hydrolytic, Thermal, and Oxidative Cleavages of Dimethylaurate(I) and Tetramethylaurate(III). *J. Am. Chem. Soc.* **1977**, *99*, 8440−8447.
(108) Weinhold, F.; Landis, C. R. Natural Bond Orbitals and Extensions of Localized Bonding Concepts. *Chem. Educ. Res. Pract.* **2001**, *2*, 91−104.
(109) The values shown are without a solvent sphere, which might be important for the highly charged species. Also a Mulliken population analysis gives rather different values, for instance a charge of −0.76 on Cu in [Cu(CF$_3$)$_4$]$^{3-}$.
(110) The free anion, long thought to exist only as a fleeting intermediate, was recently synthesized: Prakash, G. K. S.; Wang, F.; Zhang, Z.; Haiges, R.; Rahm, M.; Christe, K. O.; Mathew, T.; Olah, G. A. Long-Lived Trifluoromethanide Anion: A Key Intermediate in Nucleophilic Trifluoromethylations. *Angew. Chem., Int. Ed.* **2014**, *53*, 11575−11578.
(111) For CF$_3$ radical, an experimental structure is available from an analysis of the vibration-rotation spectrum, C-F 1.318, C−F−C angle 110.8°: Yamada, C.; Hirota, E. Infrared Diode Laser Spectroscopy of the CF$_3$ ν_3 Band. *J. Chem. Phys.* 1983, *78*, 1703−1711. Previous estimates of structural parameters are discussed in this paper.10.1063/1.444969
(112) Why I$_2$? The oxidant is more easily analyzed theoretically than O$_2$. Other authors had previously used the I$_2$ oxidant to generate the analogue [Cu(CHF$_2$)$_4$]$^-$. Eujen, R.; Hoge, B.; Brauer, D. J. Synthesis and Properties of Donor-free Bis(difluoromethyl)cadmium, (CF$_2$H)$_2$Cd NMR Spectroscopic Detection and Structure of Tetrakis(difluoromethyl)cuprate(III) and Related Compounds. *J. Organomet. Chem.* **1996**, *519*, 7−20.10.1016/S0022-328X(96)06142-6
(113) Weiss, E.; Wolfrum, R. Die Kristallstruktur des Lithiumtetramethylzinkats. *Chem. Ber.* 1968, *101*, 35−40. CSD refcode LTMEZN.10.1002/cber.19681010107
(114) Schlosser, M. Organoalkali Chemistry. In *Organometallics in Synthesis*, 3rd Manual ed.; Schlosser, M., Ed.; John Wiley & Sons, Inc.: Hoboken, NJ, 2013; p 61.
(115) Mosquera, M. E. G.; Gómez-Sal, P.; Diaz, I.; Aguirre, L. M.; Ienco, A.; Manca, G.; Mealli, C. Intriguing I$_2$ Reduction in the Iodide for Chloride Ligand Substitution at a Ru(II) Complex: Role of Mixed Trihalides in the Redox Mechanism. *Inorg. Chem.* **2016**, *55*, 283−291.
(116) Could the SP-(CF$_3$)$_4^{2-}$ unit stand alone? A full optimization was attempted, but although the system remained for several cycles on a plateau with the initial cyclic structure, it eventually converted into the dimer F$_3$C-CF$_3$ and two single CF$_3^-$ units.
(117) For a related CuPh$_3^{2-}$ in the structure of a polynuclear Cu(I) system, see Olmstead, M. M.; Power, P. P. Isolation and First Structural Characterization of Dimethyl Sulfide Solvates of Phenyllithium, Phenylcopper, and Lower and Higher order Lithium Phenylcuprate Reagents. *J. Am. Chem. Soc.* **1990**, *112*, 8008−8014.
(118) Fleming, I. *Molecular orbitals and organic chemical reactions*, student ed.; John Wiley and Sons, Ltd.: New York, 2009.
(119) Mori, S.; Nakamura, E. In *Modern Organocopper Chemistry* Krause, N., Ed.; Wiley-VCH: New York, 2002; Chapter 10.
(120) Lemal, D. M. Perspective on Fluorocarbon Chemistry. *J. Org. Chem.* **2004**, *69*, 1−11.
(121) See the references in the review of Young, A. G.; Hanton, L. R. Square Planar Silver(I) Complexes: A Rare but Increasingly Observed Stereochemistry for Silver(I). *Coord. Chem. Rev.* **2008**, *252*, 1346−1386.
(122) Dahl, E. W.; Szymczak, N. K. Hydrogen Bonds Dictate the Coordination Geometry of Copper: Characterization of a Square-Planar Copper(I) Complex. *Angew. Chem., Int. Ed.* **2016**, *55*, 3101−3015.
(123) Cheung, P. M.; Berger, R. F.; Zakharov, L. N.; Gilbertson, J. D. Square Planar Cu(I) Stabilized by a Pyridinediimine Ligand. *Chem. Commun.* **2016**, *52*, 4156−4159.
(124) The reader deserves an explanation for the apparent incongruence of these SP 18e species. Evidently, all the ligand σ hybrids are populated and yet a square planar geometry obtains. It must be that the repulsion between the populated b$_{1g}$ combination of ligands and the filled x^2-y^2 orbital, is not too great. Alternatively, one can view the σ bonding in these molecules from the perspective of hypervalency.
(125) For an angular overlap model analysis of the bonding, see ref 6.
(126) Cirera, J.; Ruiz, E.; Alvarez, S. Stereochemistry and Spin State in Four-Coordinate Transition Metal Compounds. *Inorg. Chem.* **2008**, *47*, 2871−2889.

DOI: 10.1021/acs.chemrev.6b00251
Chem. Rev. 2016, 116, 8173−8192

(127) For the relevant Walsh diagrams for a transition metal and a main group element, see ref 9, pp 199 and 445.
(128) Heinekey, D. M.; Oldham, W. J., Jr. Coordination Chemistry of Dihydrogen. *Chem. Rev.* **1993**, *93*, 913−926.
(129) Bau, R.; Drabnis, M. H. Structures of Transition Metal Hydrides Determined by Neutron Diffraction. *Inorg. Chim. Acta* **1997**, *259*, 27−50.
(130) Černý, R.; Bonhomme, F.; Yvon, K.; Fischer, P.; Zolliker, P.; Cox, D. E.; Hewat, A. Hexamagnesium Dicobalt Undecadeuteride $Mg_6Co_2D_{11}$: Containing $[CoD_4]^{5-}$ and $[CoD_5]^{4-}$ Complex Anions Conforming to the 18-electron Rule. *J. Alloys Compd.* **1992**, *187*, 233−248.
(131) Kaim, W. The Shrinking World of Innocent Ligands: Conventional and Non-Conventional Redox-Active Ligands. *Eur. J. Inorg. Chem.* **2012**, *2012*, 343−348 and references therein.
(132) Kaim, W.; Schwederski, B. Non-innocent Ligands in Bioinorganic Chemistry—An overview. *Coord. Chem. Rev.* **2010**, *254*, 1580−1588.

DOI: 10.1021/acs.chemrev.6b00251
Chem. Rev. 2016, 116, 8173−8192